Carbon Burial in T~~t~~wo Greenland Fjords: Exploring the Influence of Glacier Type on Organic Carbon Dynamics

Marius Buydens[1], Emil De Borger[1], Lorenz Meire[2,5], Samuel Bodé[3], Antonio Schirone[4], Karline Soetaert[5], Ann Vanreusel[1], Ulrike Braeckman[1,6]

[1]Marine Biology Research Group, Ghent University, Krijgslaan 281, S8 9000, Gent, Belgium
[2]Greenland Climate Research Centre, Greenland Institute of Natural Resources, Kivioq 2, 3900 Nuuk, Greenland
[3]Isotope Bioscience Laboratory (ISOFYS), Ghent University, Coupure Links 653, 9000 Ghent, Belgium
[4]ENEA, Department of Sustainability, Marine Environment Research Centre S. Teresa, Via Santa Teresa 1, 19032 Pozzuolo di Lerici, Italy
[5]Royal Netherlands Institute of Sea Research (NIOZ), Department of Estuarine and Delta Systems, Korringaweg 7, P.O. Box 140, 4401, NT, Yerseke, the Netherlands
[6]Institute of Natural Sciences, Operational Directorate Natural Environment, Vautierstraat 29, 1000, Brussels, Belgium

Correspondence to: Marius Buydens (marius.buydens@ugent.be)

Abstract. Fjord systems ~~are~~ play a crucial role in ~~for~~ the burial and long-term storage of organic carbon (OC)~~, contributing significantly to global blue carbon sequestration~~. Despite their importance, Greenland's fjords remain underrepresented in global carbon budgets, even though accelerated melt of the Ice Sheet alters these ecosystems through increased freshwater discharge and iceberg calving, ultimately leading to glaciers retreating inland. This study compares sediment TOC, TN, and Chl-a content as well as $\delta^{13}C$, $\delta^{15}N$ and organic carbon burial rates (OCBRs) in two neighbouring Greenland fjords, Nuup Kangerlua, dominated by marine-terminating glaciers (MTGs), and Ameralik, influenced by a land-terminating glacier (LTG), to explore the effects of both types of glaciers on sediment carbon dynamics. ~~This study compares organic carbon burial rates (OCBRs) in two neighbouring Greenland fjords – Nuup Kangerlua, influenced by marine-terminating glaciers (MTGs), and Ameralik, dominated by land-terminating glaciers (LTGs) – to explore the effects of both types of glaciers on sediment carbon dynamics.~~ Since subglacial discharge-driven upwelling in Nuup Kangerlua ~~(MTG)~~ has been shown to support higher summer phytoplankton blooms, we expected higher sediment ~~organic carbon~~OC content and burial in this MTG fjord. Despite different glacial regimes, the two investigated fjord systems showed similar traits with OC predominantly of marine origin and similar OCBRs of 18.0 ± 1.6 and 16.2 ± 1.7 g m^{-2} yr^{-1} in Nuup Kangerlua and Ameralik, respectively. Higher Chl-a and OC contents were recorded in the sediments of outer and mid Ameralik compared to those in Nuup Kangerlua. The results underscore that benthic – pelagic coupling in glacial fjords is complex, emphasizing the need for further research to disentangle the interactions driving primary production, food web flow, lateral and vertical OC transport, as well as OC degradation and preservation in fjord sediments. ~~However, our observations show higher OC content in sediments of Ameralik's (LTG) outer and mid fjord section and a similar OCBR in both fjords. This unexpected finding may be linked to differences in pelagic grazing pressure, organic carbon transport, and sediment preservation mechanisms. The findings call for further research to unravel the complex interactions between primary production, organic carbon transport, and preservation processes in different glacial fjord systems.~~

1 Introduction

Fjord systems ~~play a crucial role in burial and long-term storage of organic carbon~~represent significant carbon sinks, contributing to approximately a tenth of the annual ~~burial of organic blue~~ carbon ~~burial~~ (OC) (Smith et al., 2015). In the Northern hemisphere, carbon content and burial in fjord sediments have mainly been studied in Alaska (Cui et al., 2016a), Scotland and Ireland, (Smeaton et al., 2016; Smeaton and Austin, 2017; Smeaton and Austin, 2019; Smeaton et al., 2021), Norway (Duffield et al., 2017; Faust and Knies, 2019; Włodarska-Kowalczuk et al., 2019), Sweden (Placitu et al., 2024; Watts et al., 2024) and Svalbard (Kuliński et al., 2014; Koziorowska et al; 2018; Zaborska et al., 2018; Włodarska-Kowalczuk et al., 2019). In the Southern Hemisphere, estimates of OC burial in fjord systems are comparatively sparse and largely confined to a few regions, including Patagonia (Sepúlveda et al., 2011), South Georgia (Berg et al., 2021), Antarctica (Eidam et al., 2019), and New Zealand (Hinojosa et al., 2014; Cui et al., 2016b).

Despite this growing body of research in both hemispheres, Greenland remains markedly underrepresented in global carbon budgets (Smith et al., 2015), even though its coast is fringed by a myriad of fjords, including some of the most extensive fjord systems in the Arctic. ~~Nevertheless, despite the prevalence of fjords along Greenland's extensive coast, a notable gap remains in their representation in global carbon budgets (Smith et al., 2015).~~ Moreover, Greenland harbours the only remaining Arctic ice sheet since the last glacial period, which plays a key role in regulating Earth's climate and sea-level. The current accelerated melting of the Greenland Ice Sheet (King et al., 2020; Greene et al., 2024), driven by climate change, has far-reaching global implications and is altering fjord systems through increased freshwater discharge and iceberg calving (Calleja et al., 2017; Catania et al., 2020; Kanna et al., 2022).

Glaciers in polar regions either calve directly into the ocean (so called "marine-terminating glaciers", further referred to as MTGs) or terminate inland, discharging into lakes or the ocean via meltwater rivers ("land-terminating glaciers", LTGs). Fjords, inundated relict valleys carved out during previous glacial periods, often serve as channels through which these glaciers and meltwater rivers reach the ocean. Meltwater percolates down the cracks and crevices of glaciers to ultimately form sub-glacial rivers at their base (Chu, 2014). Since MTGs terminate in the ocean, this sub-glacial meltwater rises up from the bottom of the glacier within the fjord basin entraining nutrients, like nitrate, ammonium and phosphate, present in deeper water layers (Meire et al., 2017; Hopwood et al., 2018; 2020; Kanna et al., 2018; Cape et al., 2019; Halbach et al., 2019; Seifert et al., 2019~~Hopwood et al., 2020 and references therein~~). This upwelling water mass replenishes thereby essential nutrients for primary production in the surface waters, crucial for sustaining phytoplankton proliferation beyond the initial spring bloom phase. This extended bloom, running into the summer months may potentially lead to increased ~~organic carbon~~OC production within the fjord ecosystem (Kanna et al., 2022; Meire et al., 2023). Conversely, fjords receiving meltwater from LTGs lack this mechanism of upwelling, leading to a depletion of nutrients following the spring bloom period, resulting in substantially lower primary production in summer (Meire et al., 2017, 2023). Consequently, the carbon dynamics in LTG-dominated fjords may differ significantly from those observed in MTG-dominated fjords.

An important characteristic of fjord systems that enhances their capacity as carbon sinks is an elevated sedimentation rate, driven by their proximity to glaciers and rivers, along with the steep terrain of their watersheds (Syvitski, 1987). However, sedimentation rate alone is not the sole determinant of effective carbon burial (Bianchi et al., 2020). In general, the effectiveness of trapping ~~organic carbon~~OC varies among fjords and depends on (1) the productivity of the fjord waters, particularly phytoplankton growth, as well as terrestrial vegetation ~~growth~~ in the catchment, both of which are influenced by climate (e.g. fjord categories described in Włodarska-Kowalczuk et al., 2019), (2) factors affecting the settlement of ~~organic carbon (~~OC~~)~~ to the fjord's bottom sediments like~~(e.g.~~ fjord geomorphology and current dynamics~~)~~ (Gilbert et al., 2002; Erlandsson, 2008; Faust and Knies, 2019; Watts et al., 2024) and (3) factors limiting the degradation of settled OC, among which the refractory nature of OC (Koziorowska et al., 2015; Zaborska et al., 2018), sedimentation rate (Watts et al., 2024) and bottom water redox conditions (Hinojosa et al., 2014).

Findings from the limited number of biogeochemical studies focusing on Greenland fjords have sparked speculation that enhanced primary production observed in MTG-dominated fjords, driven by the upwelling effect, may lead to increased carbon ~~sequestration~~ burial in fjord sediments compared to LTG-influenced fjord systems (Meire et al., 2017; Meire et al., 2023; Stuart-Lee et al., 2023). However, there is limited data from Arctic fjords to test this hypothesis. In Svalbard, a lower OC content has been observed in the surface sediments of a LTG-fed fjord compared to two MTG-impacted fjord systems (Laufer-Meiser et al., 2021). In contrast, another study conducted in Svalbard reported a higher OC content in the surface sediments of a LTG- compared to a MTG-influenced fjord (Koziorowska et al., 2015). While the first study ascribed the observed pattern to the glacier-driven upwelling effect, the second study attributed the higher OC content to the higher proportion of terrestrially-derived organic matter versus the more degradable marine organic matter. A study comparing organic carbon burial rates (OCBR) in Arctic fjords stated that high Arctic fjords with limited glacial activity and a short phytoplankton growth period sequester lower amounts of carbon in the sediments compared to Arctic fjords with "active" glaciers and a relatively longer phytoplankton growth period (Włodarska-Kowalczuk et al., 2019).

This study aims to improve our understanding of carbon burial processes in Greenland fjord systems and provide insights that may refine estimates of their contribution to carbon burial at regional scales. In addition, we seek to gain insights in the influence of different types of Greenland fjord systems, more specifically in terms of MTG or LTG discharge influence. This knowledge is crucial for developing a comprehensive understanding of how climate change may impact the long-term carbon storage capacity of Greenland fjord systems and the potential related feedback effects on global climate systems.

~~Therefore, we compared carbon storage and burial in two neighbouring, sub-Arctic fjord systems which both feature a sill at their entrance and are subjected to similar offshore currents and similar geology in their catchments, but have a different glacier influence (MTG-dominated vs. LTG-dominated fjords).~~

2 Materials and methods

2.1 Study area

The two studied fjord systems are situated in the sub-Arctic coastal region of Southwest Greenland. Covering an area of 2,013 km^2, Nuup Kangerlua (formerly known as Godthåbsfjord) forms, with its many side branches, the largest fjord system of West Greenland (Mortensen et al., 2018). The main branch is ~190 km long. Three marine-terminating glaciers and three meltwater rivers discharge into the fjord (Mortensen et al., 2011; Fig. 1). The land-terminating glaciers release 7.5 ± 2.1 km^3 yr^{-1} of freshwater into the fjord system, while the marine-terminating glaciers supply 18.4 ± 5.8 km^3 yr^{-1} of freshwater in addition to 7–10 km^3 yr^{-1} of solid ice discharge (Van As et al., 2014; Langen et al., 2015). The seafloor morphology comprises two consecutive sills at the fjord entrance and a third sill located in the inner fjord area in front of the termini of the two innermost MTGs (Mortensen et al., 2011; Fig. 1). Inflow of dense coastal waters renews basin water masses in the main fjord basin usually from November until April (Mortensen et al., 2011, 2014, 2018). Bottom water temperatures ~~are~~ were situated between 1 and 1.5 ~~and 2~~°C in summer 2021, and 0.6 and 1.5 °C in spring 2022 (~~Mortensen et al., 2011~~Table 1).

Ameralik is situated south of Nuup Kangerlua, and has a length of around 75 km and a surface area of 400 km^2 (Stuart-Lee et al., 2023). The fjord receives most of the freshwater runoff from a meltwater river (Naujat Kuat) draining an inland glacier. Overeem et al. (2015) measured in 2012 a discharge of 0.78 km^3 yr^{-1} of Naujat Kuat into the fjord. A large sill is situated at the mouth of Ameralik and rises to 110 m water depth (Stuart-Lee et al., 2021). Being more than twice as shallow compared to the entrance sills in Nuup Kangerlua, the sill restricts inflow of relatively warmer and more saline sub-polar mode water (SPMW), resulting in ~~relatively lower~~ bottom water temperatures ~~of ~ 0~~ below 1°C (~~spring and summer 2019 data;~~ Stuart-Lee et al., 2021; Table 1). The seafloor geomorphology behind the sill consists of a series of basins with the deepest and more extensive basin situated about 20 km inwards from the main sill. Within this basin, the bathymetry plummets to a water depth of approximately 730 m.

Formatted: Superscript

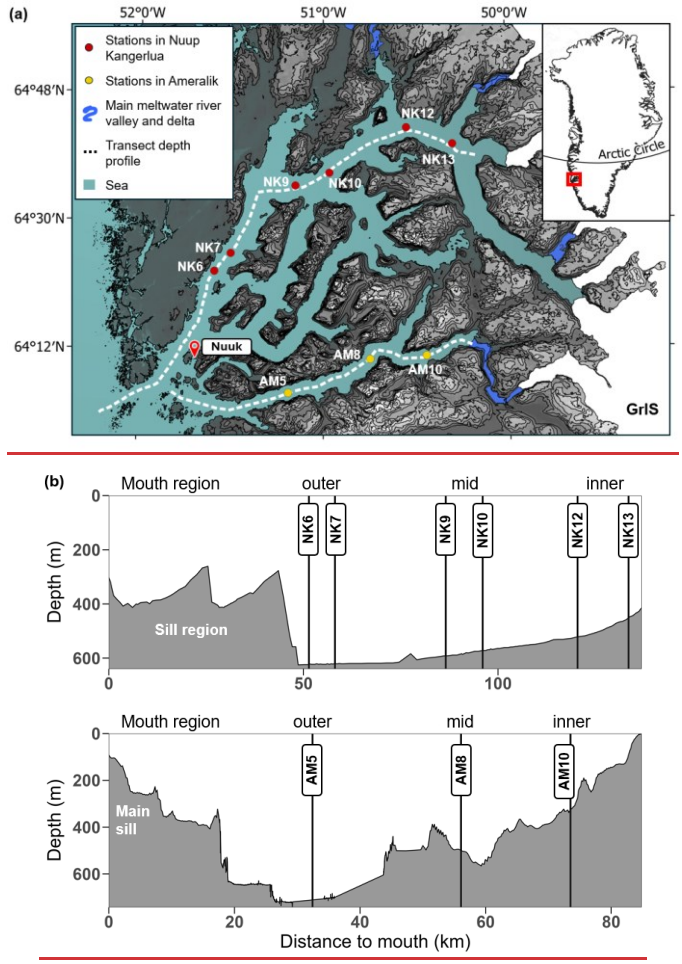

Figure 1. (a) Map showing sampling locations in Nuup Kangerlua (fed by three marine-terminating glaciers and three land-terminating glaciers) and Ameralik (receiving meltwater from a land-terminating glacier). Greenland Ice Sheet (GrIS) is depicted in white. **(b)** Water depth profiles along-axis (white dashed lines) Nuup Kangerlua (top) and Ameralik (bottom). Both fjord basins are divided in an outer, mid and inner section behind the entrance sill(s).

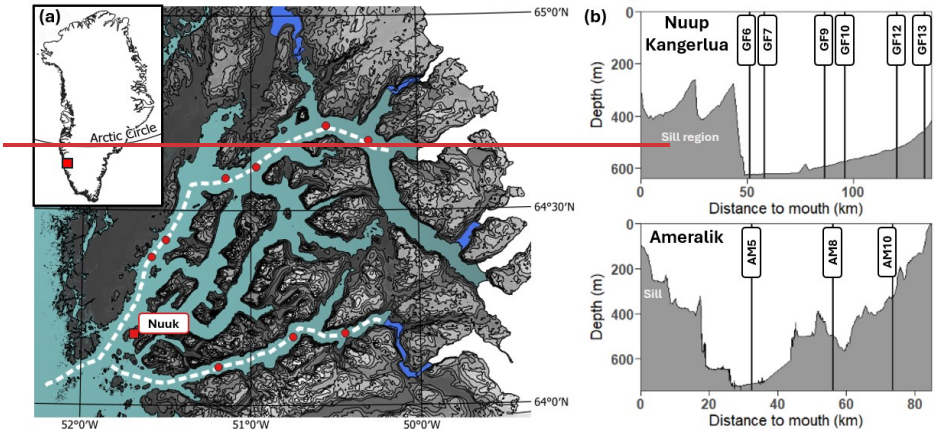

~~Figure 1: A.~~ ~~Red dots mark the locations of the sampled stations in Nuup Kangerlua (upper fjord; from mouth to head: GF6, GF7, GF9, GF10, GF12 & GF13) and Ameralik (lowermost fjord; from mouth to head: AM5, AM8 & AM10). Areas indicated in blue represent the main river valleys and deltas. Glaciers and Ice Sheet are indicated in white. White dashed lines shows the transects of the depth profiles.~~ ~~**B.**~~ ~~Water depth profiles along-axis (white dashed lines) Nuup Kangerlua (top) and Ameralik (bottom).~~

2.2 Sediment sampling

Two field campaigns were organized, one in summer 2021 and one in spring 2022. Sediment samples were taken from the research vessels *Polar Diver* (2021) and *Avataq* (2022). A UWITEC multicorer (UWITEC GmbH, Austria) was deployed to sample the seafloor and included three core liners ~~of 60 cm long~~ with an inner diameter of 8.6 cm. Stations were located along the main axis of both fjords (Fig. 1). No successful deployments could be carried out at the sill areas situated at the mouth area of both fjords due to the high abundance of gravel. Sampled stations are therefore located behind the sills, within the fjord basin. Although the mouth areas of both fjords could not be sampled, we divided each fjord basin into "outer,' "mid," and "inner" sections for clarity. Throughout the text, the terms "outer," "mid," and "inner" refer to specific station locations. For Nuup Kangerlua, the "outer" area corresponds to stations ~~GF~~NK6 and ~~GF~~NK7, the "mid" area to ~~GF~~NK9 and ~~GF~~NK10, and the "inner" area to ~~GF~~NK12 and ~~GF~~NK13. In Ameralik, the "outer", "mid", and "inner" fjord areas correspond to stations AM5, AM8, and AM10, respectively. It is important to note that earlier studies (e.g., Mortensen et al., 2011, 2014, 2018; Meire et al., 2015, 2017; Stuart-Lee et al., 2021, 2023) referred to the same stations in Nuup Kangerlua using the prefix "GF", derived from the Danish name "Godthåbsfjord". In this study, we use the prefix "NK" instead, to reflect the Greenlandic name "Nuup Kangerlua".

Formatted: Line spacing: 1,5 lines

Formatted: Font: Not Italic

Formatted: Font: Not Italic

2.2.1 Core ~~Solid phase~~ sampling and processing

At each station, three deployments were carried out for granulometry, pigment, total organic carbon (TOC) and total nitrogen (TN) analysis ~~(n = 3)~~ and one deployment for porosity and ^{210}Pb analysis ~~(n = 1)~~ and for stable isotope analysis of TOC and TN ~~(n = 1; in 2022~~. Fewer sediment stations were sampled in 2021 compared to 2022; however, bottom water temperature measurements were obtained in both years (Table 1).~~). Due to the more exploratory approach of the 2021 campaign, less stations and parameters were sampled compared to 2022 (Table 1).~~ The retrieved sediment was sliced into 1 cm ~~thick~~ slices down to 10 cm sediment depth. Sediment intended to derive sediment accumulation rates (^{210}Pb analysis) was further sliced beyond 10 cm in intervals of 2 cm until the end of the core (ranging from 10 to 44 cm sediment) ensuring sufficient material for reliable ^{210}Pb activity detection above background levels. All samples were stored at -20 °C, except for sediment samples intended for pigment analysis, which were stored at ~~-~~80 °C.

Formatted: Superscript

Table 1 Sampling dates, coordinates, water depth, and bottom water temperatures (BWT) of sampled stations in Nuup Kangerlua (~~Godthåbsfjord; GF~~NK) and Ameralik (AM).

Station	Date(s) sampled	Longitude (N)	Latitude (W)	Depth (m)	BWT (°C)	
					2021	2022
GF13	31/05/2022	64° 40.8	50° 17.3	476	1.4742	1.4135
GF12	31/08/2021 20/05/2022	64° 42.9	50° 32.8	531	1.4135	1.347
GF10	31/08/2021	64° 36.6	50° 57.5	570	1.3239	0.8074
GF9	24/05/2022	64° 33.0	51° 0.9	626	1.228	0.6737
GF7	01/09/2021 20/05/2022	64° 25.5	51° 3.4	630	1.2908	0.6387
GF6	30/08/2021	64° 22.0	51° 0.4	630	1.2791	0.6185
AM10	02/09/2021 18/05/2022	64° 11.0	50° 25.9	350	0.4943	0.4452
AM8	18/05/2022	64° 10.4	50° 45.3	488	0.5925	0.5571
AM5	03/09/2021 24/05/2022	64° 05.7	51° 11.3	730	0.5597	0.59

Station	Date(s) sampled	Longitude (N)	Latitude (W)	Depth (m)	BWT (°C)	
					2021	2022
NK13	31/05/2022	64° 40.8	50° 17.3	476	1.47	1.41
NK12	31/08/2021 20/05/2022	64° 42.9	50° 32.8	531	1.41	1.35
NK10	31/08/2021	64° 36.6	50° 57.5	579	1.32	0.81
NK9	24/05/2022	64° 33.0	51° 0.9	602	1.23	0.67
NK7	01/09/2021 20/05/2022	64° 25.5	51° 3.4	626	1.29	0.64
NK6	30/08/2021	64° 22.0	51° 0.4	630	1.28	0.62
AM10	02/09/2021 18/05/2022	64° 11.0	50° 25.9	350	0.49	0.45
AM8	18/05/2022	64° 10.4	50° 45.3	488	0.59	0.56
AM5	03/09/2021 24/05/2022	64° 05.7	51° 11.3	730	0.56	0.59

2.3 ~~Solid phase sample~~Sediment analysis

Grain size, porosity and dry bulk density were measured to provide insights into the physical structure and depositional environment of the sediment column. High porosity typically indicates fine-grained, loosely packed sediments with higher

water content, which are common in low-energy depositional environments. Conversely, lower porosity may suggest coarser, more compacted sediments, potentially reflecting higher-energy conditions or post-depositional consolidation. Grain size distribution was determined on oven-dried samples (at 60 °C for 48 h). ~~applying the laser diffraction method using a Malvern Mastersizer 2000 with Hydro 2000S module (0.02–2000 mm size range).~~ After homogenization, coarse material > 2 mm was removed by sieving. A subsample of 0.1 – 1 g was resuspended in water and analyzed using a Malvern Mastersizer 2000 with the Hydro 2000S module (size range: 0.02 – 2000 µm), which operates based on laser diffraction. The sample was sonicated for 60 s to prevent flocculation of clays before it goes through the laser. No pretreatment to remove organic or inorganic carbon was performed prior to analysis. Grain size fractions were classified according to the Wentworth scale (1922) as clay (< 4 µm), silt (4 – 63 µm), and sand (63 – 500 µm).

~~Results were categorized in clay (<4 mm), silt (4–63 mm), and sand (63–500 mm) fractions conform Wentworth scale classification (1922).~~ Sediment porosity was estimated gravimetrically using a modified water displacement method. A pre-weighed 10 ml graduated measuring cylinder was filled with 2 – 5 g of homogenized wet sediment. After addition of ultrapure water (Milli-Q) to the 10 ml mark (measured by the lower meniscus), the cylinder was weighed again. The sample was then dried at 80 °C for ~48 h and reweighed. Porosity (ϕ) was calculated based on the difference between the wet sediment weight and the dry sediment weight (i.e., the mass of porewater), recalculated to pore water volume through correction for salinity and divided by the estimated volume occupied by the sediment (calculated as 10 ml minus the volume of water added). Dry bulk density was obtained by dividing dry mass by bulk volume.

~~Porosity was obtained by dividing the porewater volume by the wet sediment volume.~~

To determine total carbon (TC), TOC and TN, sediment samples were oven-dried at 60 °C for 48 hours ground using mortar and pestle, and homogenized. Between 20 – 35 mg of dried and homogenized sediment was weighed and placed into pre-weighed silver cups. For TC and TN analysis, silver cups were sealed by folding with tweezers into compact spheres to ensure complete combustion. For TOC analysis, carbonate removal was performed by stepwise acidification: 2 – 3 drops of increasing concentrations of HCl (1%, 2%, 5%, and 10%) were added sequentially using a glass pipette. After each addition, samples were dried at 60 °C for 1 to 2 hours. This procedure was repeated over 2 – 3 days until no bubbling was observed and carbonate removal was confirmed. All measurements were conducted using a Flash 2000 NC Sediment Analyzer (Interscience), which quantifies carbon and nitrogen via dynamic flash combustion and chromatographic separation. From these data, the molar C:N ratios were calculated dividing TOC by TN and inorganic carbon (IC) was determined by subtracting TOC from TC. To investigate the origin of the organic matter (see 2.3.1), stable isotope composition, $\delta^{13}C$ (‰ deviations from V-PDB) and $\delta^{15}N$ (‰ deviations from air), was measured with an elemental analyzer (Thermo Flash EA1112 elementanalyzer) coupled to an isotope ratio mass spectrometer (Thermo Finnigan Delta V, IRMS). Prior to analysis, the same steps were followed as for TOC and TN analysis, except samples were freeze dried.

~~Samples were dried and homogenized, then analyzed for total sedimentary carbon (TC) and total nitrogen (TN). After decalcification with 37 % HCl, total organic carbon (TOC) was also measured. All measurements were conducted using a Flash 2000 NC Sediment Analyzer (Interscience). From these data, the molar CN ratios were calculated and inorganic carbon~~

Formatted: Not Highlight

Formatted: Not Highlight

Formatted: Font color: Auto

Formatted: Not Highlight

Formatted: Not Highlight

Formatted: Font: Bold, Font color: Auto

~~(IC) was determined by subtracting TOC from TC. To investigate the origin of the organic matter (see further), stable isotope composition ($\delta^{13}C$ and $\delta^{15}N$) was measured with an elemental analyzer (Thermo Flash EA1112 elementanalyzer) coupled to an isotope ratio mass spectrometer (Thermo Finnigan Delta V, IRMS).~~ To explore how glacier type affects marine primary productivity and whether and how it is incorporated in the sediment, we additionally measured, for each sediment slice, the content of chlorophyll-a (Chl-a) and of its degradation products (pheophorbide-a, and pheophytin-a, pheophorbide-a like, and pheophytin-a like following Wright and Jeffrey (1997). For pigments extraction, 2 ml acetone (90%) was added to 0.5 g freeze dried sediment under red light conditions preventing pigment degradation. The samples were subsequently sonicated for 30 s and incubated overnight at 4 °C in the dark to aid pigment release. Afterwards, the samples were centrifuged (10 min, 4000 rpm, 4 °C) and the supernatant was passed through 0.2 µm PTFE filters. Pigment separation was performed using an HPLC system (Agilent 1200 Infinity II, Agilent Technologies) equipped with a cooled auto-sampler, column oven, photodiode array detector, and fluorescence detector, following the method of Van Heukelem and Thomas (2001). Chlorophyll-a and its degradation products were identified at 665 nm wavelength. Individual pigment concentrations were determined using the response factors of the respective standards. ~~These different pigments were determined by the response factor of standard pigments as described by Van Heukelem and Thomas (2001).~~ The ratio of Chl-a to Chloroplastic Pigment Equivalent (CPE, comprising the sum of all aforementioned pigments) was used as a proxy for the "freshness" or lability of photosynthetically produced organic matter (Schubert et al., 2005; Koho et al., 2008).

Formatted: Font color: Text 1

2.3.1 Calculation of marine organic carbon fraction

Stable isotope composition in addition to C:N ratios of settled organic matter in fjord sediments has been used in multiple studies to estimate the proportion of marine versus terrestrially derived organic matter (St-Onge and Hillaire-Marcel, 2001; Hinojosa et al., 2014; Koziorowska et al., 2015; Smeaton & Austin, 2017; Zaborska et al., 2018; Faust and Knies, 2019; Limoges et al., 2020; Placitu et al., 2024). Terrestrial organic matter, primarily derived from vascular plants, tends to have higher C:N ratios (> 12) and more depleted $\delta^{13}C$ values (-25 to -30 ‰ $\delta^{13}C$) due to the dominance of lignin-rich, cellulose-based material and the use of C_3 photosynthesis pathways (Lamb et al., 2006). In contrast, marine organic matter, originating from phytoplankton and other aquatic organisms, typically shows lower C:N ratios and less negative $\delta^{13}C$ values (-18 to -24 ‰ $\delta^{13}C$), reflecting a protein-rich composition and different carbon fixation mechanisms (Lamb et al., 2006). ~~Stable isotope composition in addition to C:N ratios of settled organic matter in fjord sediments has been used in multiple studies to estimate the proportion of marine versus terrestrially derived OM (Koziorowska et al., 2015; Smeaton & Austin, 2017; Faust and Knies, 2019).~~ However, the use of solely stable isotopes can render an overestimation of marine OM as eroded and reburied fossil carbon from rocks (petrogenic carbon) display $\delta^{13}C$ values within the range of recent marine OM masking a marine fossil provenance (Burdige, 2007; Cui et al., 2016b; Wang et al., 2024). The bedrock of the catchments of both fjords is predominantly made up of Precambrian orthogneisses, granodiorites and granites. Potential sources of petrogenic carbon like meta-sedimentary rocks occur, but are rather rare in the catchment areas (< 0.1 % of exposed bedrock) (Næraa et al., 2014). Therefore, it is reasonable to assume that the input of ancient marine carbon is likely to be limited. The catchments of both

Formatted: Superscript

Formatted: Superscript

Formatted: Superscript

Formatted: Superscript

fjords consist of tundra shrub vegetation, which are typically C_3 plants. Published $\delta^{13}C$ values for terrestrial plant material in Greenland remain limited, but available data indicate a range of -33.9‰ to -26.9‰ (Thompson et al., 2018). However, due to the scarcity of $\delta^{13}C$ records specific to Greenland's marine organic matter, terrestrial vegetation and soil, we adopted end-member values from nearby Arctic and sub-Arctic systems. For the marine end-member, we used a $\delta^{13}C$ value of -20.6‰, consistent with those reported in Svalbard studies by Winkelman and Knies, and Koziorowska et al. (2015). We used the marine end-member value from Faust and Knies (2019), originally applied in sub-Arctic Norwegian fjords, as it falls within the broader $\delta^{13}C$ range of Arctic terrestrial organic matter (-35‰ to -25‰) reported by Kuliński et al. (2014).

The fraction of OC derived from terrestrial C was calculated following the formula of Thornton and McManus (1994):

$$OC_{terrestrial} = \frac{\delta^{13}C_i - \delta^{13}C_M}{\delta^{13}C_T - \delta^{13}C_M} \quad (1)$$

and

$$OC_{marine} = 1 - OC_{terrestrial}, \quad (2)$$

where $\delta^{13}C_i$ represents the surface sediment values (0 – 2 cm) of $\delta^{13}C_{org}$ of each sample, $\delta^{13}C_M$ is the marine end-member and $\delta^{13}C_T$ is the terrestrial end-member. Only the upper 0 – 2 cm was used to be able to compare with literature. ~~These end-members were adopted from Faust and Knies (2019): -19.3‰ and -26.5‰ vs. V-PDB-LSVEC, for the marine and terrestrial end-member, respectively. These end-members were derived from Northern and Mid-Norway fjord sediments and agree with western Barents Sea sediments (Knies and Martinez, 2009; Faust and Knies, 2019) and Svalbard fjord sediments (Winkelman and Knies, 2005).~~

2.4 ^{210}Pb and ^{137}Cs analysis

Lead-210 dating of the sediment was done using HPGe gamma ray spectroscopy (diameter: 101.6 mm, height 134.9 mm, carbon-epoxy window, model BE5030-7500SL-RDC-4, Canberra, Asse, Belgium). The dried and grinded sediment samples were packed into aluminium tins with calibrated geometries of 35 ml, 60 ml or 120 ml, depending on the amount of dried sediment available, and left for > 21 days after sealing allowing ingrowth equilibration of the ^{226}Ra with the proxies used to estimate its activity (^{214}Pb and ^{214}Bi) (Brenner et al. 2004). When tins could not be filled entirely, the headspace was measured accurately, and an empirical model per geometry was used to correct for change in efficiency. The measurement of ^{210}Pb activity was done using its 46.5-KeV gamma peak as described by Cutshall et al. (1983). The contribution of "supported" ^{210}Pb was assessed by estimating the ^{226}Ra activity from the average of the ^{214}Pb (at 295.2 and 351.9 keV) and ^{214}Bi (at 609.3 keV) activities. Supported ^{210}Pb was then subtracted from the total ^{210}Pb for each depth interval to determine "excess" ^{210}Pb ($^{210}Pb_{exs}$). Additionally, ^{137}Cs levels were determined through gamma spectroscopic measurement of its 661.7-KeV gamma peak.

Formatted: Subscript
Formatted: Superscript
Formatted: Superscript
Formatted: Superscript
Formatted: Superscript

2.4.1 Organic carbon burial rate ~~constant~~

Log-transformed $^{210}Pb_{ex}$ activities were plotted against cumulative dry mass depth (g cm^{-2}) for each station. Sedimentation rates at stations AM5, AM8, NK7, and NK9 were determined using the constant rate of supply (CRS) model (Appleby, 2001), as a distinct increase in ^{137}Cs was detected at these sites (Fig. A1), supporting the CRS-based chronology. The observed increase in ^{137}Cs activity is attributed to global fallout from atmospheric nuclear weapons testing, which peaked in 1963. In contrast, the CF:CS (constant flux:constant sedimentation) model (Sanchez-Cabeza and Ruiz-Fernández, 2012) was applied to stations NK10, NK12, NK13, and AM10, where the $^{210}Pb_{ex}$ profiles exhibited approximately exponential trends but lacked a clearly defined ^{137}Cs peak. For these stations, log-transformed $^{210}Pb_{ex}$ activities were plotted against cumulative dry mass depth (g cm^{-2}) for each station. As a result, the sedimentation rate estimates for these stations should be treated with caution and verified in future studies. Mass accumulation rates (MAR, kg m^{-2} yr^{-1}) were derived from the slope of the linear regression (for CF:CS) or from the CRS model output. Bulk sediment accumulation rates (SAR, mm yr^{-1}) were calculated by dividing MAR by the average bulk density at each station. Organic carbon burial rates (OCBRs) were then calculated by multiplying MAR by the TOC content at the 9 – 10 cm sediment layer. ~~Log-transformed $^{210}Pb_{xs}$ activities were plotted against the cumulative dry mass depth (g cm^{-2}) of the sediment per station. Sedimentation rates at stations GF9, GF7, AM8 and AM5 were determined using the constant rate of supply model (CSR) (Appleby, 2001), as a clear ^{137}Cs peak was measured at these stations (Fig. A1). For the stations GF13, GF12, GF10, AM10 and GF6, the sediment mass accumulation rate (MAR, kg solids cm^{-2} yr^{-1}) was derived from the slope of the linear regression according to the CF:CS model (Constant Flux:Constant Sedimentation) (Sanchez-Cabeza & Ruiz-Fernández, 2012). The bulk sediment accumulation rate (SAR, mm yr^{-1}) was calculated by dividing MAR by the average bulk density of the sediment per station. The organic carbon burial rate (OCBR) per station was determined using the MAR and the TOC content at the deepest sediment layer in common for all sediment cores (9–10 cm sediment interval depth). No bioturbated or mixed upper layer was observed in the profiles.~~

We did not apply corrections for bioturbation or mixing processes, as the $^{210}Pb_{ex}$ profiles do not show evidence of such activity in the upper sediment layers. However, these processes cannot be conclusively ruled out, particularly since some of the ^{137}Cs profiles feature broad activity peaks. Nonetheless, the ^{210}Pb-derived chronology appears to be supported by the ^{137}Cs profiles in AM5, AM8, NK7 and NK9 (Smith, 2001; Barsanti et al., 2020). The broad ^{137}Cs curves or inflections, marking sustained elevation in ^{137}Cs activity after an initial increase followed by a gradual decrease moving up the sediment column, are therefore more likely explained by continued exposure of settling particles to residual ^{137}Cs in the overlying water after 1963. As a result, younger sediment layers also contain measurable amounts of ^{137}Cs, smearing the signal across multiple horizons. This phenomenon has been observed in other marine settings (Tamburrino et al. 2019) and even in lake sediments (Drexler et al., 2018).

Formatted: Font: (Default) +Body (Times New Roman)

Formatted: Font: (Default) +Body (Times New Roman), Superscript

Formatted: Superscript

Formatted: Superscript

Formatted: Subscript

Formatted: Subscript

Formatted: Superscript

Formatted: Subscript

Formatted: Font: 10 pt

2.5 Statistical analysis

We examined differences between the two fjords and ~~between~~ among stations in terms of sedimentary TOC and TN content, C:N ratio, Chl-a content and Chl-a:CPE ratio, using data from both the upper 2 cm sediment surface and the arithmetic mean~~average~~ of the upper 10 cm sediment column. Data from summer (2021) and spring (2022) were combined and treated as replicates, as the difference between the two seasons was insignificant (Welch's ANOVA, $p > 0.05$; see further). As a consequence, stations ~~GF~~NK12, ~~GF~~NK10, ~~GF~~NK7, AM10 and AM5 have six replicates since they were sampled in both seasons, while the other stations have three replicates as those stations were only sampled during spring 2022 (Table 1). Statistical analyses were performed using one-way ANOVA. Welch's ANOVA was applied when variances were unequal, and the Kruskal-Wallis test was used when normality assumptions were violated. For significant results, post hoc comparisons were made using Tukey's test, Games-Howell test, or Dunn's test, depending on the initial method. Results are reported as means ± standard deviation. Statistical analyses were performed in R (R Core Team, 2023) using the car, rstatix and FSA packages (Fox and Weisberg, 2019; Kassambara, 2023; Ogle et al., 2023).

3 Results

3.1 ~~Solid phase~~Sediment parameters

The median grain size ($d_{0.5}$) was situated in the silt fraction for all stations, though AM5, AM8 and the top 2 cm of ~~GF~~NK7 displaying medium-sized silt, while all other stations are situated in the very fine to fine silt class (Fig. 2). In Nuup Kangerlua, the median grain size ($d_{0.5}$) exhibits a modest spatial trend from the inner to the outer fjord (Fig. 2). At the inner stations (NK13 and NK12), grain size remains relatively small (< 20 µm) and consistent with depth, reflecting a stable depositional environment dominated by fine particles. Grain size at the mid-fjord stations (NK10 and NK9) is slightly larger but still within the fine-silt range, indicating only subtle hydrodynamic variation. At the outer stations (NK7 and NK6), grain size increases slightly further and shows more variability with depth, which may reflect localized influence of bottom currents or episodic input of coarser particles near the fjord mouth. Overall, differences in grain size between stations are relatively small, but a general trend toward coarser material at the fjord's outer reaches is observable. ~~In Nuup Kangerlua, the median grain size (d0.5) shows a clear spatial pattern from the inner to the outer fjord (Fig. 2). At the inner stations (GF13 and GF12), the grain size remains relatively small (< 20 µm) and consistent with depth, reflecting a stable depositional environment dominated by fine particles. Moving to the mid-fjord stations (GF10 and GF9), there is a slight increase in grain size, though still within the fine-silt range, indicating limited hydrodynamic influence. At the outer stations (GF7 and GF6), the grain size increases further to medium-sized silt and varies with depth, suggesting the deposition of coarser sediments near the fjord mouth due to stronger currents and more dynamic conditions.~~

In Ameralik, a similar trend is observed (Fig. 2). The inner station (AM10) shows small, uniform grain sizes comparable to those at the inner stations in Nuup Kangerlua. At the mid-fjord station (AM8), the grain size increases slightly, reflecting a

Formatted: Subscript

Formatted: Subscript

subtle shift in depositional energy. The outer station (AM5) exhibits the largest grain sizes, with ~~noticeable~~ variability ~~at~~ ~~depth~~between replicates, indicating more pronounced hydrodynamic ~~sorting and energy~~conditions and fluctuations in this area. ~~-~~Porosity and dry density generally fluctuated ~~along the~~with sediment depth ~~gradient~~ without a consistent pattern across most stations.~~clear trend, except for station GF10, where porosity decreased and dry density increased with depth.~~ In contrast, station NK10 exhibited the expected trend of decreasing porosity and increasing dry density with depth. These variations appeared to be influenced by grain size, although the processes driving the trends at NK10 are less clearly linked to sediment texture.

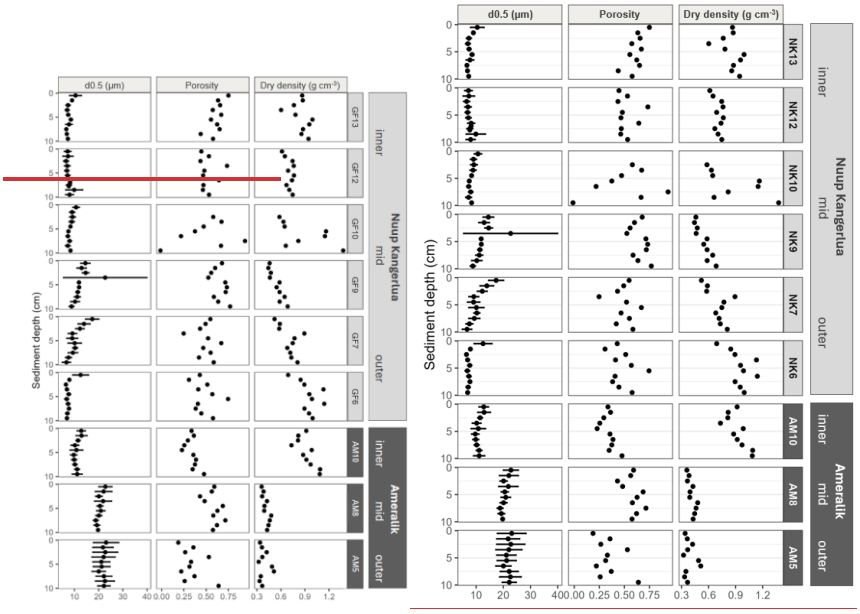

Figure 2.~~:~~ Sediment profiles of median grain size (µm), porosity and dry density (g cm~~⁻~~$^{-3}$) of Nuup Kangerlua (~~GF~~NK stations) and Ameralik (AM stations). Error bars represent SD (n = 3 for ~~GF~~NK6, ~~GF~~NK9, ~~GF~~NK13 and AM8 and n = 6 for ~~GF~~NK7, ~~GF~~NK10, ~~GF~~NK12, AM5 and AM10). Only one replicate for porosity and dry density.

In Ameralik, we observed a distinct increasing trend in the surface 2 cm sediments from the inner fjord to the mid-fjord stations for TOC, TN, Chl-a content, and the Chl-a:CPE ratio. The only exception was the C:N ratio, which decreased from the inner to the mid-fjord, and then remained relatively constant (Fig. 3). In Nuup Kangerlua, the pattern was more variable. TOC, TN, and Chl-a content rose from the inner fjord towards the mid-fjord stations, peaking at ~~GF~~NK7 and ~~GF~~NK9, but then declined at ~~GF~~NK6, ~~near~~ at the outer fjord area (Fig. 3). Unlike Ameralik, the Chl-a:CPE ratio in Nuup Kangerlua showed fluctuations

along the fjord axis, without a consistent trend. Overall, station AM5, located in the deepest part of the main basin of Ameralik, displayed the highest (Welch's ANOVA, $p < 0.05$) Chl-a (16.4 ± 2.0 µg g^{-1} DM) and CPE (45.9 ± 7.1 µg g^{-1} DM) content, as well as the highest Chl-a:CPE ratios (0.36 ± 0.04) of the top 2 cm surface sediments compared to all other sampled stations of both fjords (Fig. 3). In addition, both outer and mid stations of Ameralik displayed the highest TOC values (AM5: 2.1 ± 1.5 %; AM8:1.6 ± 0.1 %) within the upper 2 cm sediment, which were significantly higher (Welch's ANOVA, $p < 0.05$) than those observed in inner fjord station AM10 and all stations in Nuup Kangerlua (values ranging from 0.1 to 1.3 %).

Formatted: Font: Not Italic

Formatted: Font: Not Italic

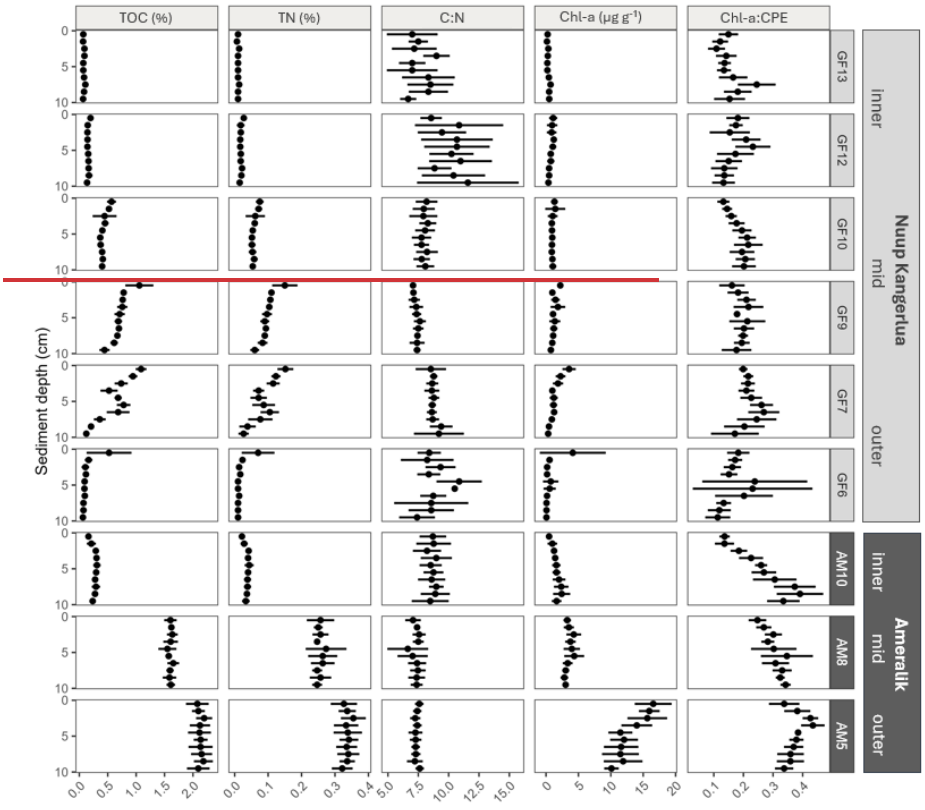
Chl-a:CPE
Chl-a (µg g⁻¹)
C:N
TN (%)
TOC (%)
Nuup Kangerlua
inner
mid
outer
GF13
GF12
GF10
GF9
GF7
GF6
Ameralik
inner
mid
outer
AM10
AM8
AM5
Sediment depth (cm)

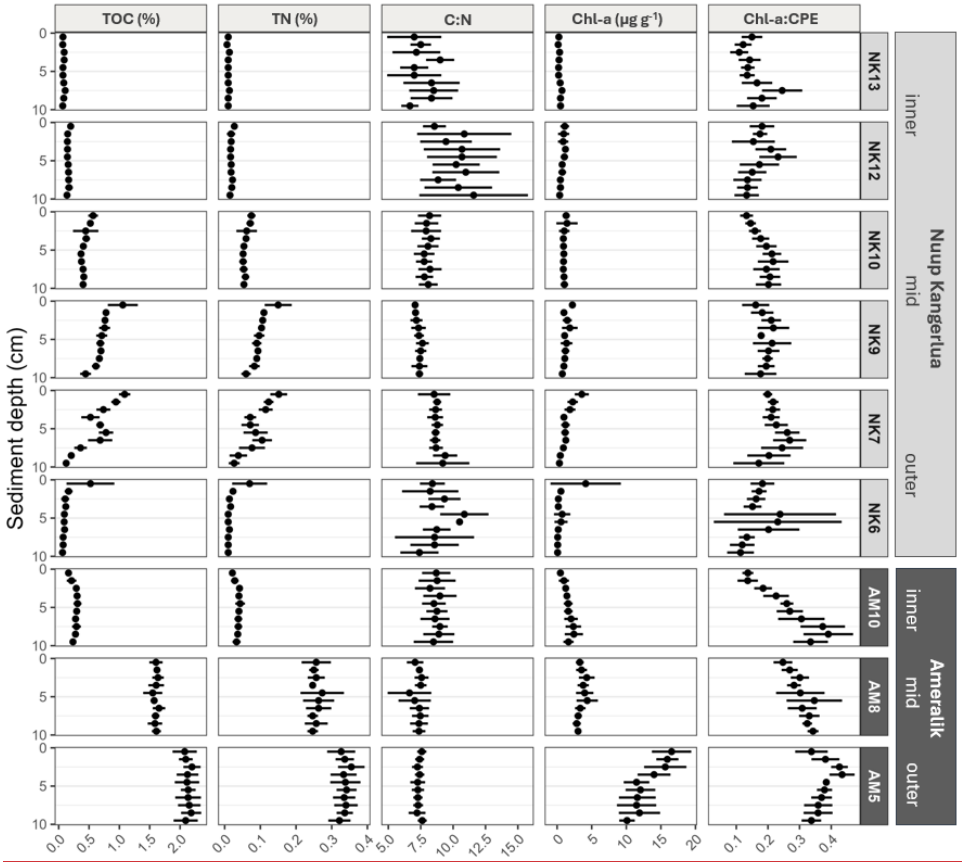

Figure 3. Vertical sediment profiles depicting TOC and TN (%), molar C:N ratios and Chl-a (µg g^{-1} DM) of the upper 10 cm sediment of Nuup Kangerlua (GFNK stations) and Ameralik (AM stations). Error bars represent SD (n = 3 for GFNK6, GFNK9, GFNK13 and AM8 and n = 6 for GFNK7, GFNK10, GFNK12, AM5 and AM10).

Apart from GFNK13, the organic carbon inOC at all stations within both fjords displayed $\delta^{13}C$ values characteristic for marine algae, ranging from -(-22.4 to -20.7 ‰). Stations NK12 and AM10, both located closer to glacial inputs, showed slightly more depleted $\delta^{13}C$ values, indicating a minor shift toward a terrestrial signal (Fig. 4). While the $\delta^{13}C$ value fluctuated widely at GFNK13 ranging from -26.3 to -23.8 ‰, indicating a stronger terrestrial influence and a more heterogeneous mixture of

Formatted: Superscript

organic matter sources. ~~while~~ Notably, $\delta^{15}N$ at this station increased consistently with depth, from 5.7 ‰ to 12.2 ‰.~~$\delta^{15}N$ consistently increased with sediment depth from 5.7 to 12.2‰~~ (Fig. A42). The depleted $\delta^{13}C$ values support enhanced mixing with terrestrial organic matter, while the elevated $\delta^{15}N$ values are more typical of marine sources, as they remain well above the 1‰ threshold commonly associated with terrestrial inputs. The absence of intensive agriculture in the region, which could otherwise lead to anthropogenic $\delta^{15}N$ enrichment, supports this interpretation (Harris & Elliot, 2019). Together, the isotopic trends at NK13 suggest a dynamic depositional setting with varying contributions from glacial runoff and in-situ marine production. ~~The more depleted $\delta^{13}C$ values at this station suggest relatively more mixing with terrestrial OM, while $\delta^{15}N$ levels are more indicative of a marine origin, since values are well above 1 ‰ and no intensive agriculture exists in the region (Harris and Elliot, 2019; Fig. 4). Levels of $\delta^{13}C$ in the upper 2 cm slightly increased from inner to outer stations within Nuup Kangerlua indicating an increasing marine influence in terms of organic carbon composition towards the outer fjord area. In Ameralik, the least depleted $\delta^{13}C$ signatures were observed in AM8.~~

Formatted: Superscript

Formatted: Superscript

Formatted: Superscript

Formatted: Superscript

Formatted: English (United States)

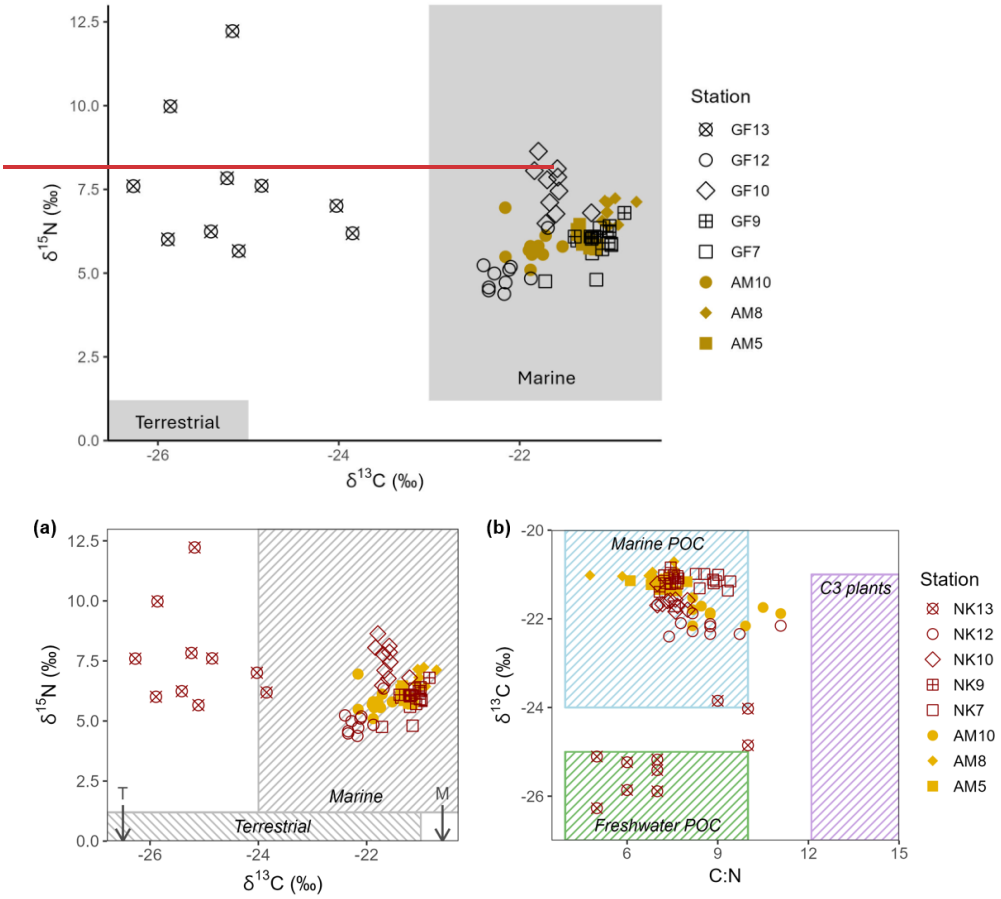

Figure 4. (a) $\delta^{13}C$ (‰ deviations from V-PDB) values plotted against $\delta^{15}N$ (‰ deviations from air) values of the POM present in the sediment for the different station of Ameralik (filled symbols) and Nuup Kangerlua (open symbols). Typical marine and terrestrial ranges of $\delta^{13}C$ (lamb et al., 2006) and $\delta^{15}N$ (Zaborska et al., 2018) are indicated with rectangles. (b) $\delta^{13}C$ plotted against C:N ratios. Ranges of marine and freshwater POC, and C3 terrestrial plants are displayed as rectangles for reference (values taken from Lamb et al., 2006). Marine (M) and terrestrial (T) $\delta^{13}C$ end-members used in this study are indicated with arrows.

~~**Figure 4:** $\delta^{13}C$ (‰ deviations from V-PDB) values plotted against $\delta^{15}N$ (‰ deviations from air) values of the POM present in the sediment for the different station of Ameralik (colored) and Nuup Kangerlua (open symbols). Typical marine and terrestrial ranges of $\delta^{13}C$ and $\delta^{15}N$ are indicated with rectangles following Zaborska et al. (2018).~~

3.2 Organic carbon burial rates

Sediment mass (MAR) and volume accumulation rates (SAR) roughly showed an increasing trend towards the inner fjord in Nuup Kangerlua. In Ameralik, MAR and SAR are also higher in the inner compared to the outer station, with minimum values in the mid station (Table 2). Burial rates of organic carbon increased towards the fjord head in Nuup Kangerlua until mid-fjord station GFNK10 where it reached the maximum observed rate (29.4 g OC m^{-2} yr^{-1}). Following station GFNK12 revealed a marked drop in OCBR (9.6 g OC m^{-2} yr^{-1}), whereafter high OCBR reappear in GFNK13 (27.5 g OC m^{-2} yr^{-1}). In Ameralik, an opposite pattern unfolded with maximum OCBR in AM5 (214.07 g OC m^{-2} yr^{-1}) and minimum rate in inner fjord AM10 (9.9 g OC m^{-2} yr^{-1}). Note that the accumulation rates at stations NK10, NK12, NK13, and AM10 are estimates based on the CF:CS model and were not validated with independent time markers (Smith 2001; Barsanti 2020). Therefore, these estimates should be confirmed in future studies.

Table 2. Mass sediment accumulation rate (MAR), bulk sediment accumulation rate (SAR) and organic carbon burial rate (OCBR) per station. The CRS method was applied at stations NK7, NK9, AM5, and AM8, while the CF:CS method was used for stations NK10, NK12, NK13, and AM10. ~~Stations are situated from mid-fjord towards the head (inner):~~ "GFNK" denotes Nuup Kangerlua and "AM" Ameralik.

Station	MAR (kg m^{-2} yr^{-1})	SAR (mm yr^{-1})	OCBR (g m^{-2} yr^{-1})
GF13	14.1 ± 3.5	15.0 ± 3.7	27.5 ± 8.3
GF12	5.9 ± 1.0	7.1 ± 1.2	9.6 ± 1.7
GF10	7.0 ± 0.1	8.3 ± 1.1	29.4 ± 4.0
GF9	3.4 ± 0.1	5.1 ± 1.4	19.1 ± 5.2
GF7	2.6 ± 0.1	3.5 ± 1.3	6.5 ± 2.7
GF6	1.8 ± 0.1	1.9 ± 0.8	1.5 ± 0.6
AM10	4.0 ± 2.8	5.2 ± 2.0	13.1 ± 5.0
AM8	1.1 ± 0.0	2.4 ± 0.0	17.2 ± 0.3
AM5	1.1 ± 0.0	2.9 ± 0.3	23.9 ± 2.3

Station	MAR (kg m^{-2} yr^{-1})	SAR (mm yr^{-1})	OCBR (g m^{-2} yr^{-1})
NK13	14.1 ± 3.5	15.0 ± 3.7	27.5 ± 8.3
NK12	5.9 ± 1.0	7.1 ± 1.2	9.6 ± 1.7
NK10	7.0 ± 0.1	8.3 ± 1.1	29.4 ± 4.0
NK9	3.1 ± 0.2	4.8 ± 0.3	17.5 ± 0.6
NK7	2.4 ± 0.2	4.1 ± 0.4	5.9 ± 0.8
AM10	4.0 ± 2.8	5.2 ± 2.0	9.9 ± 5.0
AM8	1.1 ± 0.1	2.6 ± 0.2	17.7 ± 0.3
AM5	1.0 ± 0.1	3.5 ± 0.2	21.0 ± 1.1

4 Discussion

With this study we wanted to identify to what extent the higher surface water productivity in a fjord with a MTG is reflected in carbon burial potential of the deep water sediments. We therefore expected higher OC content and OCBRs in sediments of

Nuup Kangerlua compared to Ameralik, as MTGs present in Nuup Kangerlua increase nutrient upwelling, allowing primary productivity to extend over longer periods. Indeed, earlier studies by Stuart-Lee et al. (2023) and Meire et al. (2023) noted comparable primary productivity in Nuup Kangerlua and Ameralik at the start of the productive season (April, May). Yet, with increasing meltwater discharge, a summer bloom was observed in Nuup Kangerlua which led to a greater overall phytoplankton biomass compared to Ameralik (Stuart-Lee et al., 2023; Meire et al., 2023). However, in this study, we found a higher OC content in sediments of outer and mid fjord stations AM5 and AM8 in Ameralik compared to Nuup Kangerlua. These findings are supported by observations from a gravity core sampled nearby station AM5, which also revealed similar elevated carbon content in the sediment (Møller et al., 2006). Our results therefore do not support the hypothesis of higher carbon burial potential of MTG fjords compared to LTG driven systems.

4.1 Surface sediment OC content

The OC content in the sediments of Nuup Kangerlua and Ameralik is representative for (sub-)Arctic fjord sediments (Fig. 5a). In terms of fresh organic matter, we found an average Chl-a content in Nuup Kangerlua's sediments which was slightly below the typical range observed in other North Atlantic fjords (Włodarska-Kowalczuk et al., 2019). In contrast, Ameralik exhibited an average Chl-a content nearly three times higher than the maximum values reported for Svalbard fjords (Włodarska-Kowalczuk et al., 2019). This elevated average is largely driven by the exceptionally high Chl-a content observed at station AM5.

So far, studies comparing MTG and LTG fjord systems are limited (Koziorowska et al., 2015; Laufer-Meiser et al., 2021). These studies suggest that MTG fjords tend to exhibit higher OC accumulation, as indicated by elevated OC content in surface sediments. However, when comparing the LTG system Ameralik and the MTG system Nuup Kangerlua with datasets from other fjords (Smith et al., 2002; Thamdrup et al., 2007; Koziorowska et al., 2015; Cui et al., 2016; Faust and Knies, 2019; Włodarska-Kowalczuk et al., 2019; Laufer-Meiser et al., 2021), we observed that surface sediment OC content in LTG and even non-glaciated fjords can be comparable to that of MTG systems across the (sub-)Arctic region (Fig. 5A). Nevertheless, it is important to note that LTG fjords are underrepresented in current datasets, and low-glacial-activity MTG systems may bias comparative interpretations.

These observations suggest that factors beyond glacial influence play a significant role in controlling the degree of benthic-pelagic coupling. Specifically, the presence of MTGs does not inherently result in higher OC accumulation within sediments compared to systems without subglacial upwelling. However, elevated MARs may dilute OC content with inorganic material, potentially skewing these observations. Additionally, higher TOC content in surface sediments does not automatically equate to more efficient OC burial.

Formatted: Not Highlight

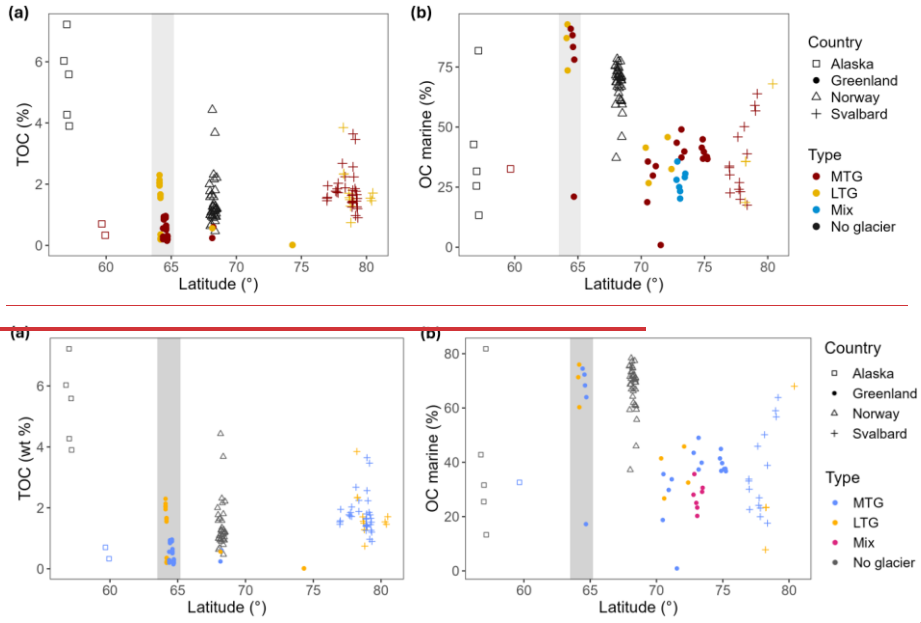

Figure 5. ~~:~~ **(a)** ~~**A.**~~ TOC content of surface sediments along latitude. Data compiled from Smith et al. (2002), Thamdrup et al. (2007), Koziorowska et al. (2015), Cui et al. (2016a); Faust and Knies (2019), Włodarska-Kowalczuk et al. (2019), Laufer-Meiser et al. (2021) and this study. ~~**(b)** **B.**~~ Fraction of TOC of marine origin along latitude. Data compiled from Koziorowska et al. (2015), Faust and Knies (2019) and this study. Both figures display data from fjords located in high latitude countries: Alaska, Greenland, Norway and Svalbard. The grey band constraints the Greenland fjords investigated in this study. Data indicated in red~~blue~~ and yellow~~red~~ represent Marine terminating-glacier (MTG) and land terminating-glacier (LTG)-influenced fjord systems, respectively. The mixed type represents fjords where the dominance of MTG(s) vs LTG(s) on the fjord's hydrology could not be differentiated from literature or satellite images are depicted in blue. Non-glacial fjords are represented in black. ~~Fjord data illustrated in grey represent fjords hosting no major glaciers within their catchments.~~ Both graphs were created following and updating the example of Faust and Knies (2019).

Formatted: English (United States)

4.2.1 OC origin

An important clue in resolving the observed patterns can be found in the deepest part of Ameralik's basin. There, specifically at station AM5, we measured a five times higher Chl-a content combined with 1.7 times higher Chl-a:CPE ratios compared to the maximum values in sediments of Nuup Kangerlua, which points to an enhanced preservation of fresh organic matter (i.e. more labile OC) within these sediments. The Chl-a content remained elevated throughout the entire 10 cm sediment profile and was consistent between spring and summer data. A difference in timing of the onset of the phytoplankton bloom between the two fjords, as previously observed (Stuart-Lee et al., 2023), could have led to an earlier build-up of pigments at the seafloor of Ameralik compared to Nuup Kangerlua at the time of sampling. However, the relatively elevated values throughout the 10 cm sediment profiles and the consistency between spring and summer data exclude such sampling time bias. In Svalbard, Koziorowska et al. (2015) also observed higher OC content in the surface sediments of a LTG-influenced fjord versus a MTG-impacted fjord. The LTG-fed fjord appeared to receive a higher fraction of terrestrial OC, which tends to be more resistant against degradation compared to marine OC (Wakeham and Canuel; 2006; Koziorowska et al., 2015). Yet, in our case, the sediment stable isotope composition and C:N ratios of both fjords reflect OC of predominantly marine origin in both fjords, likely due to the limited vegetation and a catchment geology consisting of orthogneisses, granodiorites and granites rather than organic-rich sedimentary rocks (Næraa et al., 2014) (Fig. 4; Fig. 5b). An exception is inner station NK13 in Nuup Kangerlua, which displayed $\delta^{15}N$ of marine signature, though depleted $\delta^{13}C$ values which combined with C:N values indicated a freshwater provenance (Fig. 4b). Since elevated $\delta^{15}N$ values can also be caused by degradation (Dai et al., 2005), this station may contain OM more of terrestrial origin. In contrast, the stable isotope composition found at the head of Ameralik, in front of the land-terminating glacier, does not indicate a dominant terrestrial input.

So in general, the higher OC content in Ameralik sediments is not related to increased terrestrial input in the LTG fjord compared to the MTG-dominated fjord. In fact, sediments from both fjords receive OM from predominantly marine origin.

4.2 Organic carbon burial rates

Despite the higher OC content observed in the outer and mid part of the LTG-fed fjord, OCBRs were similar in both fjords due to the relatively higher MARs in Nuup Kangerlua. The higher MARs in Nuup Kangerlua result from the substantially higher discharge that three MTGs and three LTGs generate compared to the input of a single LTG in Ameralik. The average OCBR in Nuup Kangerlua was only on average slightly higher (18.0 ± 1.6 g OC m^{-2} yr^{-1}), but not significantly, compared to Ameralik (16.2 ± 1.7 g OC m^{-2} yr^{-1}). However, it must be noted that glacial run-off induced lithogenic dilution of OC can lead to an underestimation of OCBR in Nuup Kangerlua. Nevertheless, the observed values fall within the range of sub-Arctic fjords and Arctic fjords impacted by active glaciers (Włodarska-Kowalczuk et al., 2019).

On the local scale, Meire et al. (2023) estimated that annual pelagic primary production in 2016 was approximately three times higher in a head station of Nuup Kangerlua (~90 g C m^{-2} yr^{-1} at NK10) than in a head station of Ameralik (~30 g C m^{-2} yr^{-1} at AM10). Similarly, our results show that the OCBR at this very same station NK10 was about three times higher than at AM10.

However, at basin scale, carbon burial remains similar in both fjords. These findings underscore the complexity of carbon burial dynamics in glacial fjords, highlighting that surface productivity and glacier type alone are not reliable predictors of OC burial.

4.3 Pelagic and geomorphological influence on OC burial

OC burial in fjord sediments is shaped not only by surface productivity but also by complex interactions between water column processes, fjord morphology, and bottom water conditions. There are several processes potentially at work leading to a decoupling of OC production in the water column and OC burial in the fjord sediments as discussed further and summarized in Fig. 6.

4.3.1 OC preservation conditions

Since most of the OC deposited in both fjords is of marine origin, any differences in organic matter preservation between them are likely driven by environmental conditions rather than by differences in the nature of the organic material itself. The distinct geomorphology of Ameralik and Nuup Kangerlua, particularly their differing sill depths, likely shapes bottom water temperatures and may influence organic matter preservation within the fjords. Both fjords have no anoxic deep water masses and bottom water renewal occurs every one to two years (Mortensen, 2011; Stuart-Lee et al., 2021), but bottom water temperature differs. Ameralik's shallower sill depth (~110 m) compared to Nuup Kangerlua (~200 m) restricts the inflow of warmer, saltier coastal waters (Stuart-Lee et al., 2021). Consequently, during field sampling, bottom water temperatures in Nuup Kangerlua were consistently warmer than in Ameralik, particularly in spring, with average values of 1.33 °C and 0.53 °C, respectively. The lower bottom water temperatures in Ameralik may explain the observed higher pigment and OC preservation in AM5 by reducing microbial degradation and slowing remineralization processes compared to sediments at the mouth of Nuup Kangerlua under influence of warmer waters. A comparative study of several Svalbard fjords suggested that relatively higher pigment content in sediments may be linked to lower bottom water temperatures (Krajewska et al., 2020). However, this hypothesis warrants further investigation, as Arctic microbial communities are well adapted to low temperatures, and mineralization rates below 10 °C appear to differ only minimally (Thamdrup et al., 2007; Scholze et al., 2020).

4.3.2 Transport dynamics

Besides potential differences in organic matter preservation, lateral transport may also influence the spatial distribution of OC across the seafloor. In Nuup Kangerlua, weak along-fjord gradients in sediment TOC, TN, and Chl-a content suggest dynamic currents that may redistribute OC. Estuarine and subglacial circulations, most active during melt season, can enhance OC export from inner to outer fjord (Mortensen et al., 2011; 2014; Juul-Pedersen et al., 2015).

At both fjord mouths, tidal mixing over sills drives baroclinic circulation, reintroducing nutrients into surface waters, promoting outer fjord surface productivity (Stuart-Lee et al., 2021, 2023). This aligns with higher TOC and pigment content

as well as higher Chl-a:CPE ratios in Ameralik's outer fjord sediments. In contrast, Nuup Kangerlua sediments show no similar increase in TOC and pigment content in sediments of NK6 and NK7.

Sørensen et al. (2015) proposed that high POC export in Kobbefjord, a nearby glacier-free fjord, may result from OC input from Nuup Kangerlua. A similar OC transfer might explain a higher TOC and Chl-a content in the sediments toward Ameralik's mouth. While both fjords have estuarine and baroclinic circulation, stronger subglacial upwelling in Nuup Kangerlua likely enhances OC transport efficiency towards the fjord mouth. Ameralik may thus receive OC from outside, with deep basin retention supporting OC preservation (Fig. 6). The slightly coarser grain size at Ameralik's mid and outer stations, despite their distance from glacial input, may indeed reflect input from the entrance sill. Furthermore, the topography of Ameralik with the deep depression behind the sill can promote downslope transport and sediment accumulation, resulting in the relative higher TOC and pigment content at AM5 (Hargrave and Nielsen, 1976; Wassmann et al, 1984; Erlandsson, 2008). Therefore, hydrodynamics, downslope transport, or a combination of both can decouple surface productivity from local sediment deposition.

~~In what follows, we try to substantiate these apparent contradictory results by considering organic carbon, lability, the biogeochemical context, and variations in the export mechanisms between different fjords, Furthermore, recent findings on pelagic grazing pressures in both fjords highlight the role of food-web dynamics in carbon burial dynamics.~~

~~4.1 Enhanced OC preservation~~

~~An important clue in resolving the observed patterns can be found in the deepest part of Ameralik's basin. There, at station AM5, we measured a higher Chl-a content combined with higher Chl-a:CPE ratios compared to Nuup Kangerlua, which points to an enhanced preservation of fresh organic matter within these sediments. The Chl-a content remains elevated throughout the entire 10 cm sediment profile and is consistent between spring and summer data. A difference in timing of the onset of the phytoplankton bloom between the two fjords, as previously observed (Stuart-Lee et al., 2023), could have led to an earlier build-up of pigments at the seafloor of Ameralik compared to Nuup Kangerlua at the time of sampling. However, the relatively elevated values throughout the 10 cm sediment profiles and the consistency between spring and summer data exclude such sampling bias. In Svalbard, Koziorowska et al. (2015) also observed higher OC content in the surface sediments of a LTG-influenced fjord versus a MTG-impacted fjord. The LTG-fed fjord appeared to receive a higher fraction of terrestrial OC, which tends to be more resistant against degradation compared to marine OC (Koziorowska et al., 2015). Yet, in our case, the sediment stable isotope composition and C:N ratios of both fjords reflect OC of predominantly marine origin in both fjords, likely due to the limited vegetation and similar catchment geology consisting of orthogneisses, granodiorites and granites rather than organic-rich sedimentary rocks (Næraa et al., 2014) (Fig. 4; Fig. 5B). An exception is inner station GF13 in Nuup Kangerlua, which displayed $\delta^{15}N$ and C:N ratios of marine signature, though depleted $\delta^{13}C$ values indicative of a terrestrial provenance.~~

Therefore, if a different degree in organic matter preservation occurs between the two fjords, it has to be linked to environmental conditions rather than the nature of the OC itself. Metal shielding, particularly the association of OC with iron or manganese, may be another factor influencing the preservation of sedimentary OC. Reactive iron minerals such as iron- and manganese(oxyhydr)oxides preferentially bind to marine organic matter, forming complexes that enhance the protection of OC from microbial degradation and remineralization (Faust et al., 2022; Moore et al., 2023). Such carbon-iron and -manganese interactions have been found to persist over geological timescales, thereby enhancing long-term carbon sequestration (Faust et al., 2021; Moore et al., 2023; Wang et al., 2024). Indeed, the Greenland Ice Sheet acts as a major source of Fe and Mn to its surrounding fjords through both subglacial and glacial river discharge (Bhatia et al., 2013; Hawkings et al., 2014; 2020). Studies conducted in Nuup Kangerlua and Ameralik revealed that both fjords receive substantial amounts of Fe and Mn from (sub)glacial river inflow, which appears to be captured within the fjord basin rather than being exported offshore (Hopwood et al., 2016; Krause et al., 2021; van Genuchten 2021; 2022). Higher Fe and Mn concentrations were measured in the surface waters of inner Ameralik compared to Nuup Kangerlua, but similar concentrations appeared towards the outer area of both fjords (Krause et al., 2021; van Genuchten 2022). However, no information is available on the concentration of solid Fe and Mn particles or derived complexes in the basin sediments. Moreover, differences in the balance and interplay between sedimentation rate, influx of organic matter and Fe and Mn species, the reactivity of Fe and Mn and the depth of sulphate reduction can play a role in differences in preservation of OC (Wehrmann et al. 2014; Michaud et al., 2020; Herbert et al., 2021; Laufer-Meiser et al., 2021). This complexity, however, goes beyond the scope of this study. Hence, it is not clear if metal shielding plays a role in elevated OC and Chl-a content in Ameralik's deep basin sediments.

The distinct geomorphology of Ameralik and Nuup Kangerlua, particularly their differing sill depths, likely shapes bottom water temperatures and may influence organic matter preservation within the fjords. Both fjords have no anoxic deep water masses and bottom water renewal occurs every one to two years (Mortensen, 2011; Stuart-Lee et al., 2021), but bottom water temperature differs. Ameralik's shallower sill depth (~110 m) compared to Nuup Kangerlua (~200 m) restricts the inflow of warmer, saltier coastal waters (Stuart-Lee et al., 2021). As a result, Ameralik's deep waters (below 400 m) are around zero degrees and about one to two degrees colder than in Nuup Kangerlua (Stuart-Lee et al., 2021), which may cause the observed higher pigment preservation in AM5.

4.2 OC transport dynamics

In addition to potential differences in organic matter preservation, lateral transport can also play a role in shaping the spatial distribution of OC across the seafloor. In Nuup Kangerlua, a weak along-fjord gradient in sedimentary TOC, TN, and Chl-a content suggests a dynamic current regime that may facilitate OC redistribution. Meire et al. (2023) reported a threefold higher primary production rate at station GF10 compared to AM10 due to the summer bloom. Yet, we observe that this higher productivity did not translate into significant differences in sedimentary Chl-a and TOC content between these stations.

Although it must be noted that both parameters were relatively higher (although not significantly) at GF10 compared to AM10 and that TOC and Chl-a content at GF10 may have been diluted by the observed higher MAR.

Nuup Kangerlua's estuarine and subglacial circulations, which become most active during the melt season, may enhance OC export from the inner fjord to outer areas (Mortensen et al., 2011; 2014; Juul-Pedersen et al., 2015). Despite this potential for export in the surface waters, sediment trap data from Luostarinen et al. (2020) at GF10 (300 m depth) indicate a MAR and TOC flux comparable to the calculated OCBR. This suggests either efficient preservation of OC settling beyond 300 m or contributions from an additional OC source.

Tidal mixing at the mouths of both Nuup Kangerlua and Ameralik interacts with the sill topography, creating a density gradient that drives intermediate baroclinic circulation (Mortensen et al., 2011; Stuart-Lee et al., 2021). This circulation, characterized by out-fjord flow at depth and in-fjord flow near the surface, reintroduces nutrients to shallower layers, promoting phytoplankton growth in the outer sections of both fjords (Stuart-Lee et al., 2023). In Ameralik, this local productivity likely accounts for the higher pigment and OC content observed in the outer fjord compared to the inner region. However, the absence of similar Chl-a and TOC trends at outer stations GF6 and GF7 in Nuup Kangerlua remains unexplained.

Sørensen et al. (2015) suggested that the observed discrepancy between local primary production and the significantly higher POC export to the sediments in Kobbefjord – a small, glacier-free fjord located between Nuup Kangerlua and Ameralik – could be due to an influx of OC from Nuup Kangerlua. Similarly, part of the OC produced in Nuup Kangerlua may be imported into Ameralik, contributing to increasing TOC and Chl-a content toward Ameralik's mouth. Both fjords exhibit estuarine and intermediate baroclinic circulation (Stuart-Lee et al., 2021), but OC transport efficiency appears greater in Nuup Kangerlua due to strong upwelling driven by subglacial discharge (Mortensen et al., 2014). Consequently, Ameralik may experience net OC import, with deep basin retention and settlement of OC potentially promoting enhanced preservation (Fig. 6). However, a lack of current velocity data for Ameralik limits the ability to fully assess OC transport dynamics.

Still, the observed slightly coarser grain-size fraction in Ameralik's outer and mid fjord stations may signal an input of material from the mouth area as this station is located too far from the glacier input to reveal coarser sediment compared to the inner part of the fjord. Sea Ice and icebergs which could transport coarser material further from the source are absent in the fjord nor is there a debris flow apparent from the grain-size and ^{210}Pb profiles (Fig. A1). The coarser material may therefore originate from the entrance sill indicating a more important deep water inflow compared to Nuup Kangerlua.

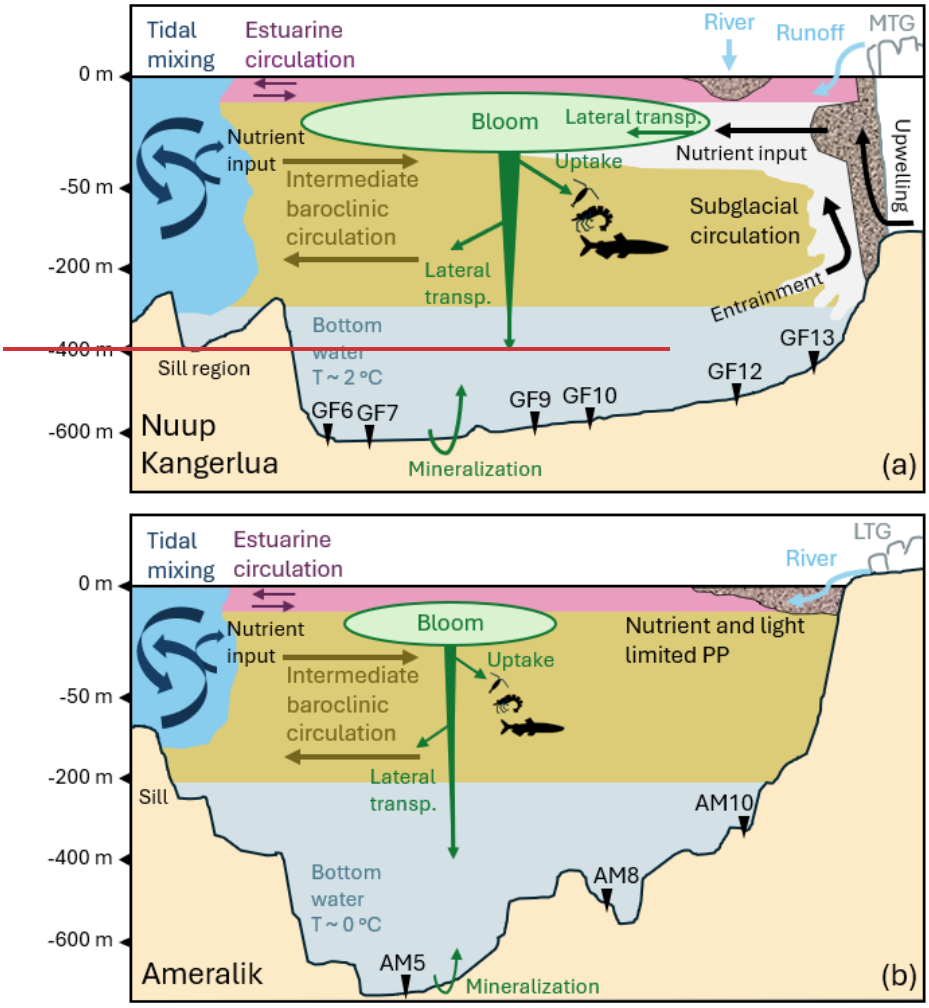
Tidal mixing
Estuarine circulation
River
Runoff
MTG
0 m
-50 m
-200 m
-400 m
-600 m
Bloom
Lateral transp.
Nutrient input
Uptake
Nutrient input
Upwelling
Intermediate baroclinic circulation
Subglacial circulation
Lateral transp.
Entrainment
Bottom water
T ~ 2 °C
Sill region
GF13
GF12
GF6
GF7
GF9
GF10
Nuup Kangerlua
Mineralization
(a)
Tidal mixing
Estuarine circulation
LTG
River
0 m
-50 m
-200 m
-400 m
-600 m
Nutrient input
Bloom
Nutrient and light limited PP
Uptake
Intermediate baroclinic circulation
Lateral transp.
Sill
AM10
AM8
Bottom water
T ~ 0 °C
AM5
Ameralik
Mineralization
(b)

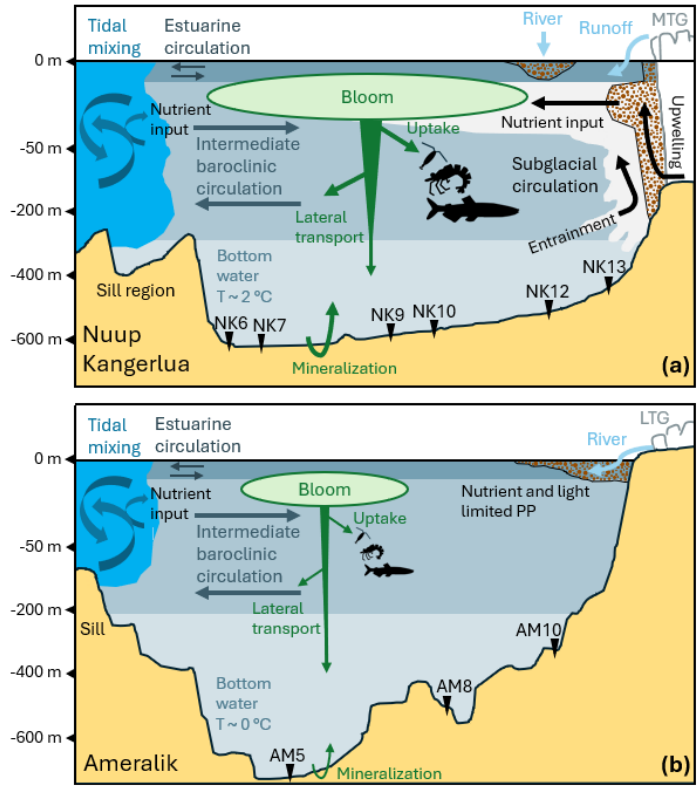

Figure 6. Schematic cross-sectional view of current regime and possible ways of phytoplankton or OC flow during summer in Nuup Kangerlua (**A**) and Ameralik (**B**) fjord systems. Tidal mixing above the sill area, estuarine circulation and intermediate baroclinic circulation occurs in both fjord systems, while the presence of MTGs in Nuup Kangerlua drives subglacial circulation through subglacial discharge. Nutrients are brought to the euphotic zone via tidal mixing and subglacial circulation. Turbid plumes, indicative of suspended sediment and organic matter input from glacier discharge and river runoff, are represented by the ~~shaded~~ brown dotted ~~pattern~~texture. Green arrows represent phytoplankton or OC transport and remineralization of organic carbon at the sediment-water interface. A larger arrow points to higher expected flows. Station locations are marked along the fjords. The current dynamics illustrated for

Nuup Kangerlua are based on Mortensen et al. (2018) and Stuart-Lee et al. (2023), while those for Ameralik are derived from Stuart-Lee et al. (2021; 2023).

4.3.3 Food web OC uptake

As both fjords exhibit a high contribution of marine-derived OC compared to other Arctic fjord systems (Fig. 5B), the unexpectedly higher sediment OC content in Ameralik's basin may reflect differences in carbon cycling pathways, both within sediments (stronger temperature-driven preservation, see 4.3.1) and in the overlying water column. In Nuup Kangerlua, greater phytoplankton biomass and a larger size class may support a more complex and efficient food web compared to Ameralik (Meire et al., 2023; Stuart-Lee et al., 2023), resulting in more OC being consumed or remineralized before it reaches the seafloor (Fig. 6). This is further supported by differences in zooplankton composition: Nuup Kangerlua hosts a higher proportion of large herbivorous copepods during the summer bloom, while smaller omnivorous taxa dominate in Ameralik (Stuart-Lee et al., 2024). However, despite these community differences, total zooplankton biomass did not differ significantly between fjords, possibly due to elevated predation pressure on larger zooplankton in Nuup Kangerlua (Stuart-Lee et al., 2024). Elevated halibut landings in MTG-influenced fjords (Meire et al., 2017), combined with the known role of MTG fronts as productive foraging zones in Svalbard (Lydersen et al., 2014; Urbanski et al., 2017; Vacquié-Garcia et al., 2018; Hamilton et al., 2019), lend further support to the hypothesis that OC transfer through higher trophic levels is intensified in Nuup Kangerlua. This enhanced trophic transfer likely reduces vertical OC export, contributing to the lower sediment OC content observed despite higher pelagic productivity.

4.4 Recommendations for future research

The expected link between elevated surface primary production in MTG-influenced fjords and OCBR was not observed. Future studies should therefore examine the mechanisms controlling this mismatch between pelagic productivity and sediment burial. In addition, our results imply that glacial influence is not necessarily the most important factor steering OCBR, which means that more Greenland fjord systems should be studied to better understand the effect of retreating MTGs on OC burial. Based on our results we identified the following avenues for future research:

- Mass accumulation rates and OCBRs need to be studied in Greenlandic and other Arctic fjords, ideally applying the CRS method, for standardized comparisons. As not all of our MARs could be determined by the CRS method, these estimates should be verified in the future.
- Accurate carbon budget construction requires integrated knowledge of primary production, zooplankton grazing, pelagic and benthic biomass as well as pelagic and benthic mineralization rates (Spilling et al., 2019), which are

Formatted: Line spacing: 1,5 lines, Outline numbered + Level: 1 + Numbering Style: Bullet + Aligned at: 0,63 cm + Tab after: 1,27 cm + Indent at: 1,27 cm

currently limited or lacking for these fjord systems. These parameters help quantify the mismatch between OC production and burial, which may arise from lateral transport processes or from OC incorporation into higher trophic levels. To address this, a more comprehensive understanding of food web dynamics and carbon flow in both fjords is essential.

- An understanding of benthic OC cycling is important for quantifying carbon turnover at the sediment-water interface, potentially revealing processes that drive differences in OC burial efficiency in different fjord systems.

~~**4.3 Food web OC flow**~~

~~As both fjords exhibit a high contribution of marine-derived OC compared to other Arctic fjord systems (Fig. 5B), the unexpectedly higher sediment OC content in the basin of Ameralik may be linked to differences in carbon cycling pathways, not only within the sediments, but potentially also above the seafloor. It is possible that the greater biomass and larger size class of phytoplankton in Nuup Kangerlua drive a more extensive and efficient food web (Meire et al., 2023; Stuart-Lee et al., 2023). As a result, a larger portion of OC is channelled into trophic transfer and remineralization, thereby reducing the amount of OC reaching the seafloor compared to Ameralik (Fig 6).~~

~~As a consequence of the summer bloom, Nuup Kangerlua has a higher proportion of large herbivorous copepods, while smaller omnivorous species dominate in Ameralik (Stuart-Lee et al., 2024). However, despite these differences in primary producers and composition of zooplankton communities, Stuart-Lee et al. (2024) found no significant difference in zooplankton biomass between the two fjords during the entire melting season. This lack of difference may be influenced by the sampling methods used, as the plankton net in that study was not optimal for capturing larger and more agile zooplankton such as krill (Stuart-Lee et al., 2024), which have been previously recorded in high abundances in the mid and inner part of the fjord (Agersted et al., 2011; Agersted & Nielsen, 2014). Another explanation may be that predation pressure exerts a control on the biomass of the larger and more zooplankton in Nuup Kangerlua (Stuart-Lee et al., 2024). Observations of higher Halibut landings in MTG-compared to LTG-influenced fjords in Greenland (Meire et al., 2017), as well as the importance of MTG fronts as foraging spots for birds and mammals as observed in Svalbard (Lydersen et al., 2014; Urbanski et al., 2017; Vacquié-Garcia et al., 2018; Hamilton et al., 2019), suggest an important transfer of OC through various trophic levels in Nuup Kangerlua. The higher consumption of OC in the water column of Nuup Kangerlua might as such impact the vertical OC transfer to the sediment and result in lower OC content in the sediment of this fjord.~~

~~**4.4 Organic carbon burial rates**~~

~~Despite the higher organic carbon content observed in the outer and mid part of the LTG-fed fjord, organic carbon burial rates were similar in both fjords. The average OCBR in Ameralik was only slightly, but not significantly, higher (16.5 ± 1.7 gC m~~

~~$^{2}yr^{-1}$) compared to Nuup Kangerlua (14.1 ± 1.6 gC $m^{-2}yr^{-1}$) and fall within the range of Sub-Arctic fjords and Arctic fjords impacted by active glaciers (Włodarska-Kowalczuk et al., 2019). The higher MAR rates in Nuup Kangerlua result from the substantially higher discharge that three MTGs and three LTGs generate compared to the input of a single LTG in Ameralik. Apparently, there is no one-on-one relationship between glacier type and OCBR. Interestingly, despite known differences in pelagic primary production, carbon burial remains similar in both fjords, likely due to limited degradation of organic carbon in Ameralik relative to Nuup Kangerlua. Thus, while the amount and type of glaciers influence both primary production and MAR, the net effect on OCBR appears to be minimal.~~

5 Conclusion

This study provides new insights into carbon burial processes in two southwest Greenland fjords with a different type of glacier influence. Our findings point to complex processes at work regarding carbon burial as our data revealed a different pattern than generally assumed in literature (Hopwood et al., 2020). Our data show that primary production generates most of the organic matter ending up at the seabed sediments in two sub-Arctic fjords with similar metamorphic and igneous catchment geology. Despite the upwelling mechanism in place sustaining more primary production, this process does not seem to induce a higher OC burial in the seabed sediments of a MTG-impacted fjord compared to a LTG-fed fjord. In contrast, this upwelling could be responsible for an export of carbon out the fjord or promoting the transfer of carbon through a more extensive food-web. In that case, MTGs ~~do~~ could function as carbon pumps where an important part of the produced OC is stored beyond the fjord basin sediments. However, differences in geomorphology or bottom water characteristics between the two fjords can also override the importance of the subglacial nutrient supply and lead to a higher preservation of the OC in the fjord sediments.~~.~~ Our findings highlight the importance of investigating both the pelagic as benthic compartment of Greenland fjord systems, which are understudied and underrepresented in global carbon budgets compared to other regions. Although this study advances our understanding of the carbon dynamics in Greenland fjords, several unresolved questions remain. For example, the role of physical circulation patterns in redistributing OC as well as differences in diagenetic processes between MTG- and LTG-influenced fjords~~, along with the role of physical circulation patterns in redistributing OC~~, require further investigation. Additionally, the potential for complex food webs and ~~higher~~ more intense trophic interactions in MTG fjords to influence carbon sequestration deserves more attention.

Understanding the driving mechanisms of OCBR in fjord systems is essential to predict the impact of climate change on OC sequestration as MTGs evolve to LTGs. The similar OCBR observed between systems suggests that the retreat of MTGs from fjords may not necessarily reduce carbon burial, as new conditions influencing OCBR will emerge. Nevertheless, when assessing the impact of climate change on OC burial budgets, it is crucial to consider the fate of OC produced within the fjord.

Appendix A

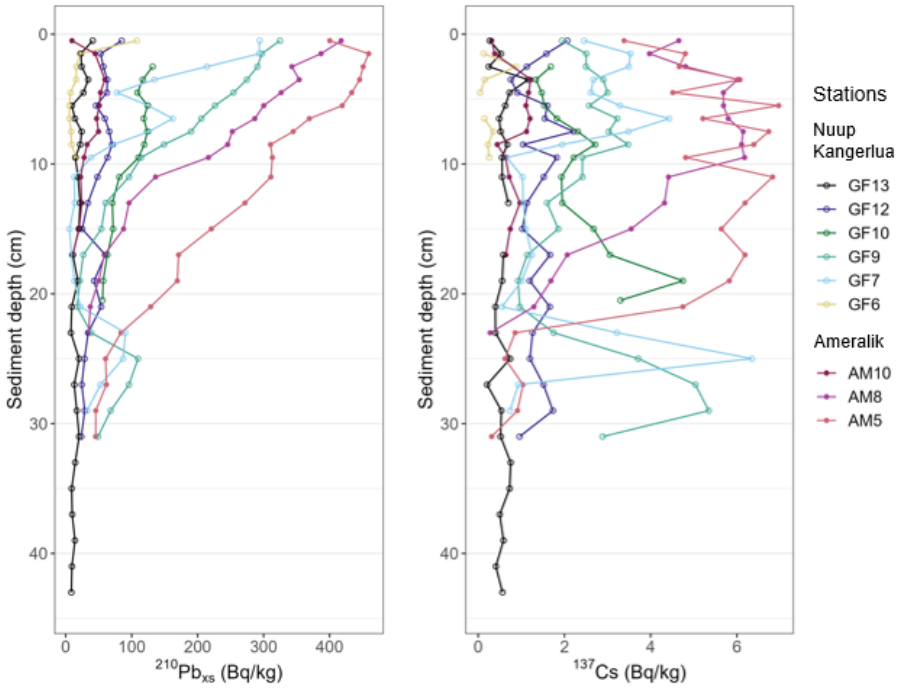

Figure: A1. Excess ^{210}Pb and ^{137}Cs profiles of Nuup Kangerlua stations (~~GF~~NK13, ~~GF~~NK12, ~~GF~~NK10, ~~GF~~NK9, ~~GF~~NK7 and ~~GF~~NK6) and Ameralik stations (AM10, AM8 and AM5).

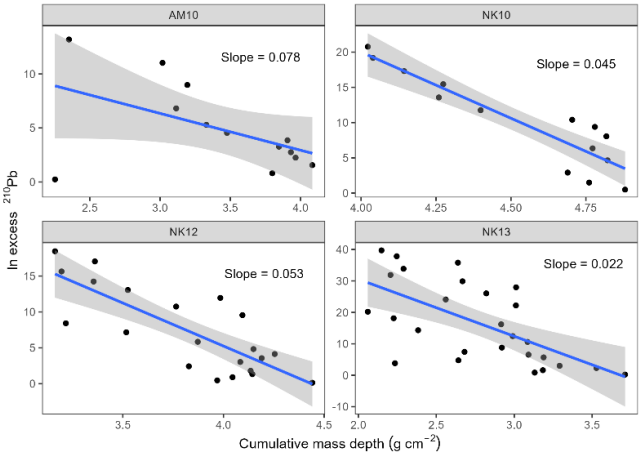

Figure A2. The natural logarithm of the activity of $^{210}Pb_{ex}$ is plotted against the cumulative mass depth with the linear blue line representing CF:CS fitting for stations AM10, NK10, 12 and 13.

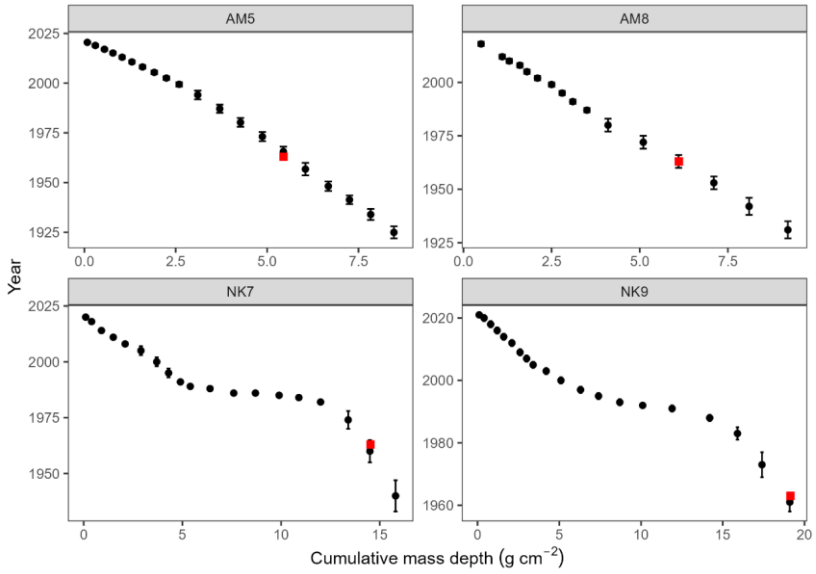

Figure A3. Age–depth models for sediment cores from stations AM5, AM8, NK7, and NK9, constructed using the Constant Rate of Supply (CRS) model based on $^{210}Pb_{ex}$ activity. Black circles represent modeled sediment ages plotted against cumulative mass depth (g cm^{-2}), with error bars showing ±1σ uncertainties. Red squares indicate the depth of the ^{137}Cs activity peak (1963), used as an independent chronological marker for model validation.

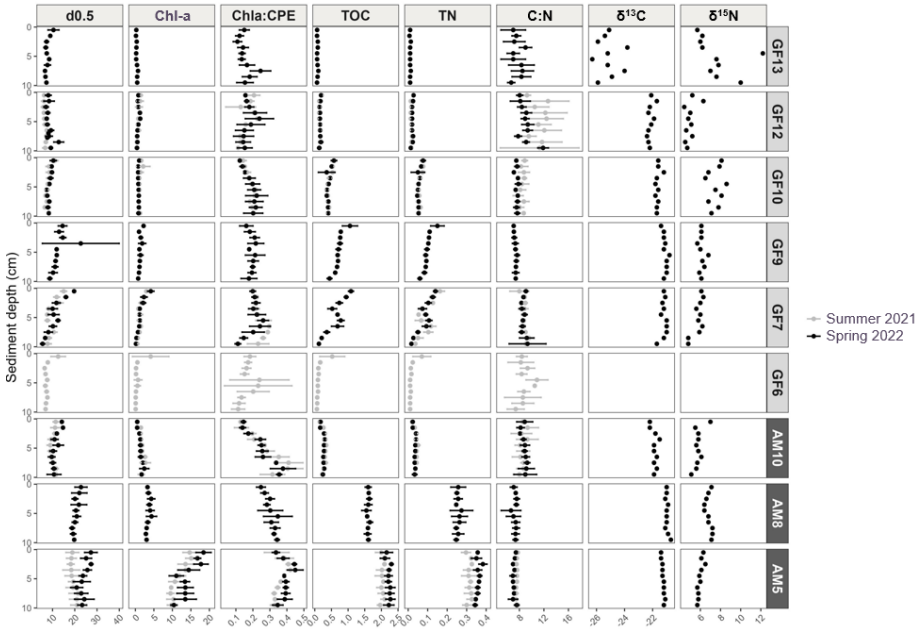

Figure A42.: Vertical sediment profiles depicting average median grain size (µm), Chl-a content (µg g^{-1} DM), Chl-a:CPE ratio, TOC and TN (%), and molar C:N ratios, and single core values of $\delta^{13}C$ (‰), $\delta^{15}N$ (‰), porosity and dry density (g cm^{-3}) of the upper 10 cm sediment of Nuup Kangerlua (stations ~~GF~~NK13, ~~GF~~NK12, ~~GF~~NK10, ~~GF~~NK9, ~~GF~~NK7 and ~~GF~~NK6) and Ameralik (stations AM10, AM8, AM5). Error bars represent SE (n = 3). ~~Orange~~ Grey and black colors represent end of summer 2021 and spring 2022, respectively. Data from the two seasons is available for stations ~~GF~~NK12, ~~GF~~NK7, AM10 and AM5.

Author contribution

LM, AVR, KS and UB acquired funding for the research project and developed the overall research objectives. LM, MB, UB, AVR, KS and EDB contributed during the field work. SB supervised and carried out lab analyses of Pb^{210} and Cs^{137}. MB conducted formal analysis and AS assisted in MAR calculations and interpretation. MB prepared the original draft and all authors reviewed the manuscript.

Competing interests

The authors declare that they have no conflict of interest.

Acknowledgements

Our sincere thanks to the Greenland Institute of Natural Resources for providing access to lab facilities and the research vessel *Avataq*, as well as accommodations during fieldwork. Special appreciation goes to Captain Peter Rosvig Pedersen and the crew of the *Polar Diver* for their assistance during field sampling. We thank MSc students Charles Makio, Marianne Lollevier and Tran Manh Quan for their contributions to sample processing and preparation. We acknowledge Bart Beuselinck and Bruno Vlaeminck (Ghent University, Marine Biology Research Group) and Peter Van Breughel (NIOZ) for sample analysis. OpenAI's ChatGPT was used to check for grammar and improve the readability of the manuscript.

Financial support

This work is part of the IMAGIN project, funded by Research Foundation-Flanders (FWO) (grant no 3G043120). The research leading to results presented in this publication was carried out with infrastructure funded by EMBRC Belgium - FWO international research infrastructure *I001621N*.

References

Aciego, S. M., Stevenson, E. I., and Arendt, C. A.: Climate versus geological controls on glacial meltwater micronutrient production in southern Greenland, Earth And Planetary Science Letters, 424, 51–58, https://doi.org/10.1016/j.epsl.2015.05.017, 2015.

Agersted, M. D. and Nielsen, T. G.: Krill diversity and population structure along the sub-Arctic Godthåbsfjord, SW Greenland, Journal Of Plankton Research, 36, 800–815, https://doi.org/10.1093/plankt/fbt139, 2014.

Agersted, M. D., Nielsen, T. G., Munk, P., Vismann, B., and Arendt, K. E.: The functional biology and trophic role of krill (Thysanoessa raschii) in a Greenlandic fjord, Marine Biology, 158, 1387–1402, https://doi.org/10.1007/s00227-011-1657-z, 2011.

Appleby, P. G.: Chronostratigraphic techniques in recent sediments, in: Kluwer Academic Publishers eBooks, 171–203, https://doi.org/10.1007/0-306-47669-x_9, 2005.

Barsanti, M., Garcia-Tenorio, R., Schirone, A., Rozmaric, M., Ruiz-Fernández, A. C., Sanchez-Cabeza, J. A., and Osvath, I.: Challenges and limitations of the ^{210}Pb sediment dating method: Results from an IAEA modelling interlaboratory comparison exercise, Quaternary Geochronology, 59, 101093, https://doi.org/10.1016/j.quageo.2020.101093, 2020.

Berg, S., Jivcov, S., Kusch, S., Kuhn, G., White, D., Bohrmann, G., Melles, M., en Rethemeyer, J.: Increased petrogenic and biospheric organic carbon burial in sub-Antarctic fjord sediments in response to recent glacier retreat, Limnology And Oceanography, 66, 4347–4362, https://doi.org/10.1002/lno.11965, 2021.

Formatted: English (United Kingdom)

Bhatia, M. P., Kujawinski, E. B., Das, S. B., Breier, C. F., Henderson, P. B., and Charette, M. A.: Greenland meltwater as a significant and potentially bioavailable source of iron to the ocean, Nature Geoscience, 6, 274–278, https://doi.org/10.1038/ngeo1746, 2013.

Bianchi, T. S., Arndt, S., Austin, W. E. N., Benn, D. I., Bertrand, S., Cui, X., Faust, J. C., Koziorowska-Makuch, K., Moy, C. M., Savage, C., Smeaton, C., Smith, R. W., en Syvitski, J.: Fjords as Aquatic Critical Zones (ACZs), Earth-Science Reviews, 203, 103145, https://doi.org/10.1016/j.earscirev.2020.103145, 2020.

Brenner, M., Schelske, C. L., and Kenney, W. F.: Inputs of dissolved and particulate226Ra to lakes and implications for210Pb dating recent sediments, Journal Of Paleolimnology, 32, 53–66, https://doi.org/10.1023/b:jopl.0000025281.54969.03, 2004.

Burdige, D. J.: Preservation of Organic Matter in Marine Sediments: Controls, Mechanisms, and an Imbalance in Sediment Organic Carbon Budgets?, ChemInform, 38, https://doi.org/10.1002/chin.200720266, 2007.

Calleja, M. Ll., Kerhervé, P., Bourgeois, S., Kędra, M., Leynaert, A., Devred, E., Babin, M., and Morata, N.: Effects of increase glacier discharge on phytoplankton bloom dynamics and pelagic geochemistry in a high Arctic fjord, Progress in Oceanography, 159, 195–210, https://doi.org/10.1016/j.pocean.2017.07.005, 2017.

Catania, G. A., Stearns, L. A., Moon, T. A., Enderlin, E. M., and Jackson, R. H.: Future Evolution of Greenland's Marine-Terminating Outlet Glaciers, Journal Of Geophysical Research Earth Surface, 125, https://doi.org/10.1029/2018jf004873, 2019.

Chu, V. W.: Greenland ice sheet hydrology, Progress in Physical Geography Earth And Environment, 38, 19–54, https://doi.org/10.1177/0309133313507075, 2013.

Cui, X., Bianchi, T. S., Jaeger, J. M., and Smith, R. W.: Biospheric and petrogenic organic carbon flux along southeast Alaska, Earth And Planetary Science Letters, 452, 238–246, https://doi.org/10.1016/j.epsl.2016.08.002, 2016a.

Cui, X., Bianchi, T. S., Savage, C., and Smith, R. W.: Organic carbon burial in fjords: Terrestrial versus marine inputs, Earth And Planetary Science Letters, 451, 41–50, https://doi.org/10.1016/j.epsl.2016.07.003, 2016b.

Cutshall, N. H., Larsen, I. L., and Olsen, C. R.: Direct analysis of 210Pb in sediment samples: Self-absorption corrections, Nuclear Instruments And Methods in Physics Research, 206, 309–312, https://doi.org/10.1016/0167-5087(83)91273-5, 1983.

Daidu, F.: Summary of Processes and Significance of Clay Minerals in Marine Sedimentary Organic Matter Preservation and in Global Carbon Cycle, Advances in Earth Science, 2006.

Drexler, J. Z., Fuller, C. C., and Archfield, S.: The approaching obsolescence of ^{137}Cs dating of wetland soils in North America, Quaternary Science Reviews, 199, 83–96, https://doi.org/10.1016/j.quascirev.2018.08.028, 2018.

Duffield, C., Alve, E., Andersen, N., Andersen, T., Hess, S., and Strohmeier, T.: Spatial and temporal organic carbon burial along a fjord to coast transect: A case study from Western Norway, The Holocene, 27, 1325–1339, https://doi.org/10.1177/0959683617690588, 2017.

Formatted: English (United States)

Formatted: English (United States)

Eidam, E. F., Nittrouer, C. A., Lundesgaard, Ø., Homolka, K. K., en Smith, C. R.: Variability of Sediment Accumulation Rates in an Antarctic Fjord, Geophysical Research Letters, 46, 13271–13280, https://doi.org/10.1029/2019gl084499, 2019.

Faust, J. C. and Knies, J.: Organic matter sources in North Atlantic fjord sediments, Geochemistry Geophysics Geosystems, 20, 2872–2885, https://doi.org/10.1029/2019gc008382, 2019.

Faust, J. C., Tessin, A., Fisher, B. J., Zindorf, M., Papadaki, S., Hendry, K. R., Doyle, K. A., and März, C.: Millennial scale persistence of organic carbon bound to iron in Arctic marine sediments, Nature Communications, 12, https://doi.org/10.1038/s41467-020-20550-0, 2021.

Faust, J. C., Ascough, P., Hilton, R. G., Stevenson, M. A., Hendry, K. R., and März, C.: New evidence for preservation of contemporary marine organic carbon by iron in Arctic shelf sediments, Environmental Research Letters, 18, 014006, https://doi.org/10.1088/1748-9326/aca780, 20232.

Fox, J. and Weisberg, S.: An R Companion to Applied Regression, 3rd Edn., Sage, Thousand Oaks, CA, 2019. [Available at: https://www.john-fox.ca/Companion/]

Gilbert, R., Nielsen, N., Möller, H., Desloges, J. R., and Rasch, M.: Glacimarine sedimentation in Kangerdluk (Disko Fjord), West Greenland, in response to a surging glacier, Marine Geology, 191, 1–18, https://doi.org/10.1016/s0025-3227(02)00543-1, 2002.

Greene, C. A., Gardner, A. S., Wood, M., and Cuzzone, J. K.: Ubiquitous acceleration in Greenland Ice Sheet calving from 1985 to 2022, Nature, 625, 523–528, https://doi.org/10.1038/s41586-023-06863-2, 2024.

Hamilton, C. D., Vacquié-Garcia, J., Kovacs, K. M., Ims, R. A., Kohler, J., and Lydersen, C.: Contrasting changes in space use induced by climate change in two Arctic marine mammal species, Biology Letters, 15, 20180834, https://doi.org/10.1098/rsbl.2018.0834, 2019.

Harris, A. J. T. and Elliott, D. A.: Stable Isotope Studies of North American Arctic Populations: A Review, Open Quaternary, 5, 11, https://doi.org/10.5334/oq.67, 2019.

Hawkings, J. R., Wadham, J. L., Tranter, M., Raiswell, R., Benning, L. G., Statham, P. J., Tedstone, A., Nienow, P., Lee, K., and Telling, J.: Ice sheets as a significant source of highly reactive nanoparticulate iron to the oceans, Nature Communications, 5, https://doi.org/10.1038/ncomms4929, 2014.

Hawkings, J. R., Skidmore, M. L., Wadham, J. L., Priscu, J. C., Morton, P. L., Hatton, J. E., Gardner, C. B., Kohler, T. J., Stibal, M., Bagshaw, E. A., Steigmeyer, A., Barker, J., Dore, J. E., Lyons, W. B., Tranter, M., and Spencer, R. G. M.: Enhanced trace element mobilization by Earth's ice sheets, Proceedings Of The National Academy Of Sciences, 117, 31648–31659, https://doi.org/10.1073/pnas.2014378117, 2020.

Herbert, L. C., Zhu, Q., Michaud, A. B., Laufer-Meiser, K., Jones, C. K., Riedinger, N., Stooksbury, Z. S., Aller, R. C., Jørgensen, B. B., and Wehrmann, L. M.: Benthic iron flux influenced by climate-sensitive interplay between organic carbon availability and sedimentation rate in Arctic fjords, Limnology And Oceanography, 66, 3374–3392, https://doi.org/10.1002/lno.11885, 2021.

Formatted: English (United Kingdom)

Hinojosa, J. L., Moy, C. M., Stirling, C. H., Wilson, G. S., and Eglinton, T. I.: Carbon cycling and burial in New Zealand's fjords, Geochemistry Geophysics Geosystems, 15, 4047–4063, https://doi.org/10.1002/2014gc005433, 2014.

Hopwood, M. J., Connelly, D. P., Arendt, K. E., Juul-Pedersen, T., Stinchcombe, M. C., Meire, L., Esposito, M., and Krishna, R.: Seasonal Changes in Fe along a Glaciated Greenlandic Fjord, Frontiers in Earth Science, 4, https://doi.org/10.3389/feart.2016.00015, 2016.

Hopwood, M. J., Carroll, D., Dunse, T., Hodson, A., Holding, J. M., Iriarte, J. L., Ribeiro, S., Achterberg, E. P., Cantoni, C., Carlson, D. F., Chierici, M., Clarke, J. S., Cozzi, S., Fransson, A., Juul-Pedersen, T., Winding, M. H. S., and Meire, L.: Review article: How does glacier discharge affect marine biogeochemistry and primary production in the Arctic?, The Cryosphere, 14, 1347–1383, https://doi.org/10.5194/tc-14-1347-2020, 2020.

Juul-Pedersen, T., Arendt, K., Mortensen, J., Blicher, M., Søgaard, D., and Rysgaard, S.: Seasonal and interannual phytoplankton production in a sub-Arctic tidewater outlet glacier fjord, SW Greenland, Marine Ecology Progress Series, 524, 27–38, https://doi.org/10.3354/meps11174, 2015.

Kanna, N., Sugiyama, S., Ando, T., Wang, Y., Sakuragi, Y., Hazumi, T., Matsuno, K., Yamaguchi, A., Nishioka, J., and Yamashita, Y.: Meltwater Discharge From Marine-Terminating Glaciers Drives Biogeochemical Conditions in a Greenlandic Fjord, Global Biogeochemical Cycles, 36, https://doi.org/10.1029/2022gb007411, 2022.

Kassambara, A.: rstatix: Pipe-Friendly Framework for Basic Statistical Tests, R package version 0.7.2, 2023, available at: https://rpkgs.datanovia.com/rstatix/., last access: June 2024.

Kennedy, M. J. and Wagner, T.: Clay mineral continental amplifier for marine carbon sequestration in a greenhouse ocean, Proceedings Of The National Academy Of Sciences, 108, 9776–9781, https://doi.org/10.1073/pnas.1018670108, 2011.

King, M. D., Howat, I. M., Candela, S. G., Noh, M. J., Jeong, S., Noël, B. P. Y., Van Den Broeke, M. R., Wouters, B., and Negrete, A.: Dynamic ice loss from the Greenland Ice Sheet driven by sustained glacier retreat, Communications Earth & Environment, 1, https://doi.org/10.1038/s43247-020-0001-2, 2020.

Knies, J. and Martinez, P.: Organic matter sedimentation in the western Barents Sea region: terrestrial and marine contribution based on isotopic composition and organic nitrogen content, Norw. J. Geol., 89, 79–89, 2009.

Koho, K. A., García, R., De Stigter, H. C., Epping, E., Koning, E., Kouwenhoven, T. J., en Van Der Zwaan, G. J.: Sedimentary labile organic carbon and pore water redox control on species distribution of benthic foraminifera: A case study from Lisbon–Setúbal Canyon (southern Portugal), Progress in Oceanography, 79, 55–82, https://doi.org/10.1016/j.pocean.2008.07.004, 2008.

Koziorowska, K., Kuliński, K., and Pempkowiak, J.: Sedimentary organic matter in two Spitsbergen fjords: Terrestrial and marine contributions based on carbon and nitrogen contents and stable isotopes composition, Continental Shelf Research, 113, 38–46, https://doi.org/10.1016/j.csr.2015.11.010, 2015.

Krause, J., Hopwood, M. J., Höfer, J., Krisch, S., Achterberg, E. P., Alarcón, E., Carroll, D., González, H. E., Juul-Pedersen, T., Liu, T., Lodeiro, P., Meire, L., and Rosing, M. T.: Trace Element (Fe, Co, Ni and Cu) Dynamics Across the Salinity Gradient in Arctic and Antarctic Glacier Fjords, Frontiers in Earth Science, 9, https://doi.org/10.3389/feart.2021.725279, 2021.

Kuliński, K., Kędra, M., Legeżyńska, J., Gluchowska, M., and Zaborska, A.: Particulate organic matter sinks and sources in high Arctic fjord, Journal Of Marine Systems, 139, 27–37, https://doi.org/10.1016/j.jmarsys.2014.04.018, 2014.

Lalonde, K., Mucci, A., Ouellet, A., en Gélinas, Y.: Preservation of organic matter in sediments promoted by iron, Nature, 483, 198–200, https://doi.org/10.1038/nature10855, 2012.

Langen, P. L., Mottram, R. H., Christensen, J. H., Boberg, F., Rodehacke, C. B., Stendel, M., Van As, D., Ahlstrøm, A. P., Mortensen, J., Rysgaard, S., Petersen, D., Svendsen, K. H., Aðalgeirsdóttir, G., and Cappelen, J.: Quantifying Energy and Mass Fluxes Controlling Godthåbsfjord Freshwater Input in a 5-km Simulation (1991–2012)*,+, Journal Of Climate, 28, 3694–3713, https://doi.org/10.1175/jcli-d-14-00271.1, 2015.

Laufer-Meiser, K., Michaud, A. B., Maisch, M., Byrne, J. M., Kappler, A., Patterson, M. O., Røy, H., and Jørgensen, B. B.: Potentially bioavailable iron produced through benthic cycling in glaciated Arctic fjords of Svalbard, Nature Communications, 12, https://doi.org/10.1038/s41467-021-21558-w, 2021.

Limoges, A., Weckström, K., Ribeiro, S., Georgiadis, E., Hansen, K. E., Martinez, P., Seidenkrantz, M., Giraudeau, J., Crosta, X., en Massé, G.: Learning from the past: Impact of the Arctic Oscillation on sea ice and marine productivity off northwest Greenland over the last 9,000 years, Global Change Biology, 26, 6767–6786, https://doi.org/10.1111/gcb.15334, 2020.

Luostarinen, T., Ribeiro, S., Weckström, K., Sejr, M., Meire, L., Tallberg, P., and Heikkilä, M.: An annual cycle of diatom succession in two contrasting Greenlandic fjords: from simple sea-ice indicators to varied seasonal strategists, Marine Micropaleontology, 158, 101873, https://doi.org/10.1016/j.marmicro.2020.101873, 2020.

Lydersen, C., Assmy, P., Falk-Petersen, S., Kohler, J., Kovacs, K. M., Reigstad, M., Steen, H., Strøm, H., Sundfjord, A., Varpe, Ø., Walczowski, W., Weslawski, J. M., and Zajaczkowski, M.: The importance of tidewater glaciers for marine mammals and seabirds in Svalbard, Norway, Journal Of Marine Systems, 129, 452–471, https://doi.org/10.1016/j.jmarsys.2013.09.006, 2013.

Maslin, M. A. and Swann, G. E. A.: Isotopes In Marine Sediments, in: Developments in paleoenvironmental research, 227–290, https://doi.org/10.1007/1-4020-2504-1_06, 2006.

Meire, L., Søgaard, D. H., Mortensen, J., Meysman, F. J. R., Soetaert, K., Arendt, K. E., Juul-Pedersen, T., Blicher, M. E., and Rysgaard, S.: Glacial meltwater and primary production are drivers of strong CO₂ uptake in fjord and coastal waters adjacent to the Greenland Ice Sheet, Biogeosciences, 12, 2347–2363, https://doi.org/10.5194/bg-12-2347-2015, 2015.

Meire, L., Mortensen, J., Meire, P., Juul-Pedersen, T., Sejr, M. K., Rysgaard, S., Nygaard, R., Huybrechts, P., and Meysman, F. J. R.: Marine-terminating glaciers sustain high productivity in Greenland fjords, Global Change Biology, 23, 5344–5357, https://doi.org/10.1111/gcb.13801, 2017.

Formatted: English (United Kingdom)

Meire, L., Paulsen, M. L., Meire, P., Rysgaard, S., Hopwood, M. J., Sejr, M. K., Stuart-Lee, A., Sabbe, K., Stock, W., and Mortensen, J.: Glacier retreat alters downstream fjord ecosystem structure and function in Greenland, Nature Geoscience, 16, 671–674, https://doi.org/10.1038/s41561-023-01218-y, 2023.

Michaud, A. B., Laufer, K., Findlay, A., Pellerin, A., Antler, G., Turchyn, A. V., Røy, H., Wehrmann, L. M., and Jørgensen, B. B.: Glacial influence on the iron and sulfur cycles in Arctic fjord sediments (Svalbard), Geochimica Et Cosmochimica Acta, 280, 423–440, https://doi.org/10.1016/j.gca.2019.12.033, 2020.

Møller, H. S., Jensen, K. G., Kuijpers, A., Aagaard-Sørensen, S., Seidenkrantz, M. -s., Prins, M., Endler, R., and Mikkelsen, N.: Late-Holocene environment and climatic changes in Ameralik Fjord, southwest Greenland: evidence from the sedimentary record, The Holocene, 16, 685–695, https://doi.org/10.1191/0959683606hl963rp, 2006.

Moore, O. W., Curti, L., Woulds, C., Bradley, J. A., Babakhani, P., Mills, B. J. W., Homoky, W. B., Xiao, K.-Q., Bray, A. W., Fisher, B. J., Kazemian, M., Kaulich, B., Dale, A. W., and Peacock, C. L.: Long-term organic carbon preservation enhanced by iron and manganese, Nature, 621, 312–317, https://doi.org/10.1038/s41586-023-06325-9, 2023.

Mortensen, J., Lennert, K., Bendtsen, J., and Rysgaard, S.: Heat sources for glacial melt in a sub-Arctic fjord (Godthåbsfjord) in contact with the Greenland Ice Sheet, Journal Of Geophysical Research Atmospheres, 116, https://doi.org/10.1029/2010jc006528, 2011.

Mortensen, J., Bendtsen, J., Lennert, K., and Rysgaard, S.: Seasonal variability of the circulation system in a west Greenland tidewater outlet glacier fjord, Godthåbsfjord (64°N), Journal Of Geophysical Research Earth Surface, 119, 2591–2603, https://doi.org/10.1002/2014jf003267, 2014.

Mortensen, J., Rysgaard, S., Arendt, K. E., Juul-Pedersen, T., Søgaard, D. H., Bendtsen, J., and Meire, L.: Local Coastal Water Masses Control Heat Levels in a West Greenland Tidewater Outlet Glacier Fjord, Journal Of Geophysical Research Oceans, 123, 8068–8083, https://doi.org/10.1029/2018jc014549, 2018.

Næraa, T., Kemp, A. I. S., Scherstén, A., Rehnström, E. F., Rosing, M. T., and Whitehouse, M. J.: A lower crustal mafic source for the ca. 2550 Ma Qôrqut Granite Complex in southern West Greenland, Lithos, 192–195, 291–304, https://doi.org/10.1016/j.lithos.2014.02.013, 2014.

Ogle, D. H., Doll, J. C., Wheeler, A. P., and Dinno, A.: FSA: Simple Fisheries Stock Assessment Methods, R package version 0.9.5, 2023, available at: https://CRAN.R-project.org/package=FSA, last access: June 2024.

Overeem, I., Hudson, B., Welty, E., Mikkelsen, A., Bamber, J., Petersen, D., Lewinter, A. and Hasholt, B.: River inundation suggests ice-sheet runoff retention, Journal Of Glaciology, 61, 776–788, https://doi.org/10.3189/2015jog15j012, 2015.

Placitu, S., Van de Velde, S. J., Hylén, A., Hall, P. O. J., Robertson, E. K., Eriksson, M., Leermakers, M., Mehta, N., and Bonneville, S.: Limited Organic Carbon Burial by the Rusty Carbon Sink in Swedish Fjord Sediments, Journal Of Geophysical Research Biogeosciences, 129, https://doi.org/10.1029/2024jg008277, 2024.

R Core Team: R: A Language and Environment for Statistical Computing, R Foundation for Statistical Computing, Vienna, Austria, available at: https://www.R-project.org/.

Raiswell, R., Tranter, M., Benning, L. G., Siegert, M., De'ath, R., Huybrechts, P., and Payne, T.: Contributions from glacially derived sediment to the global iron (oxyhydr)oxide cycle: Implications for iron delivery to the oceans, Geochimica Et Cosmochimica Acta, 70, 2765–2780, https://doi.org/10.1016/j.gca.2005.12.027, 2006.

Sanchez-Cabeza, J. A. and Ruiz-Fernández, A. C.: 210Pb sediment radiochronology: An integrated formulation and classification of dating models, Geochimica Et Cosmochimica Acta, 82, 183–200, https://doi.org/10.1016/j.gca.2010.12.024, 2012.

Seifert, M., Hoppema, M., Burau, C., Elmer, C., Friedrichs, A., Geuer, J. K., John, U., Kanzow, T., Koch, B. P., Konrad, C., Van Der Jagt, H., Zielinski, O., and Iversen, M. H.: Influence of Glacial Meltwater on Summer Biogeochemical Cycles in Scoresby Sund, East Greenland, Frontiers in Marine Science, 6, https://doi.org/10.3389/fmars.2019.00412, 2019.

Sepúlveda, J., Pantoja, S., and Hughen, K. A.: Sources and distribution of organic matter in northern Patagonia fjords, Chile (~44–47°S): A multi-tracer approach for carbon cycling assessment, Continental Shelf Research, 31, 315–329, https://doi.org/10.1016/j.csr.2010.05.013, 2010.

Schubert, C. J., Niggemann, J., Klockgether, G., en Ferdelman, T. G.: Chlorin Index: A new parameter for organic matter freshness in sediments, Geochemistry Geophysics Geosystems, 6, https://doi.org/10.1029/2004gc000837, 2005.

Smeaton, C. and Austin, W. E. N.: Sources, Sinks, and Subsidies: Terrestrial Carbon Storage in Mid-latitude Fjords, Journal Of Geophysical Research Biogeosciences, 122, 2754–2768, https://doi.org/10.1002/2017jg003952, 2017.

Smeaton, C. and Austin, W. E. N.: Where's the Carbon: Exploring the Spatial Heterogeneity of Sedimentary Carbon in Mid-Latitude Fjords, Frontiers in Earth Science, 7, https://doi.org/10.3389/feart.2019.00269, 2019.

Smeaton, C., Austin, W. E. N., Davies, A. L., Baltzer, A., Abell, R. E., and Howe, J. A.: Substantial stores of sedimentary carbon held in mid-latitude fjords, Biogeosciences, 13, 5771–5787, https://doi.org/10.5194/bg-13-5771-2016, 2016.

Smeaton, C., Yang, H., and Austin, W. E. N.: Carbon burial in the mid-latitude fjords of Scotland, Marine Geology, 441, 106618, https://doi.org/10.1016/j.margeo.2021.106618, 2021.

Smith, J. N.: Why should we believe ^{210}Pb sediment geochronologies?, *Journal of Environmental Radioactivity*, **55**, 121–123, https://doi.org/10.1016/S0265-931X(01)00110-2, 2001.

Smith, R. W., Bianchi, T. S., Allison, M., Savage, C., and Galy, V.: High rates of organic carbon burial in fjord sediments globally, Nature Geoscience, 8, 450–453, https://doi.org/10.1038/ngeo2421, 2015.

Sørensen, H., Meire, L., Juul-Pedersen, T., De Stigter, H., Meysman, F., Rysgaard, S., Thamdrup, B., and Glud, R.: Seasonal carbon cycling in a Greenlandic fjord: an integrated pelagic and benthic study, Marine Ecology Progress Series, 539, 1–17, https://doi.org/10.3354/meps11503, 2015.

St-Onge, G. and Hillaire-Marcel, C.: Isotopic constraints of sedimentary inputs and organic carbon burial rates in the Saguenay Fjord, Quebec, Marine Geology, 176, 1–22, https://doi.org/10.1016/s0025-3227(01)00150-5, 2001.

Formatted: English (United Kingdom)

Stuart-Lee, A., Møller, E. F., Winding, M., Van Oevelen, D., Hendry, K. R., and Meire, L.: Contrasting copepod community composition in two Greenland fjords with different glacier types, Journal Of Plankton Research, https://doi.org/10.1093/plankt/fbae060, 2024.

Stuart-Lee, A. E., Mortensen, J., Van Der Kaaden, A. -s., and Meire, L.: Seasonal Hydrography of Ameralik: A Southwest Greenland Fjord Impacted by a Land-Terminating Glacier, Journal Of Geophysical Research Oceans, 126, https://doi.org/10.1029/2021jc017552, 2021.

Stuart-Lee, A. E., Mortensen, J., Juul-Pedersen, T., Middelburg, J. J., Soetaert, K., Hopwood, M. J., Engel, A., and Meire, L.: Influence of glacier type on bloom phenology in two Southwest Greenland fjords, Estuarine Coastal And Shelf Science, 284, 108271, https://doi.org/10.1016/j.ecss.2023.108271, 2023.

Tamburrino, S., Passaro, S., Barsanti, M., Schirone, A., Delbono, I., Conte, F., Delfanti, R., Bonsignore, M., Del Core, M., Gherardi, S., en Sprovieri, M.: Pathways of inorganic and organic contaminants from land to deep sea: The case study of the Gulf of Cagliari (W Tyrrhenian Sea), The Science Of The Total Environment, 647, 334–341, https://doi.org/10.1016/j.scitotenv.2018.07.467, 2019.

Thamdrup, B., Glud, R. N., and Hansen, J. W.: Benthic carbon cycling in Young Sound, Northeast Greenland, Meddelelser Om Grønland Bioscience, 58, 138–157, https://doi.org/10.7146/mogbiosci.v58.142646, 2007.

Thompson, H. A., White, J. R., and Pratt, L. M.: Spatial variation in stable isotopic composition of organic matter of macrophytes and sediments from a small Arctic lake in west Greenland, Arctic Antarctic And Alpine Research, 50, https://doi.org/10.1080/15230430.2017.1420282, 2018.

Thornton, S. F. and McManus, J.: Application of Organic Carbon and Nitrogen Stable Isotope and C/N Ratios as Source Indicators of Organic Matter Provenance in Estuarine Systems: Evidence from the Tay Estuary, Scotland, Estuarine Coastal And Shelf Science, 38, 219–233, https://doi.org/10.1006/ecss.1994.1015, 1994.

Urbanski, J. A., Stempniewicz, L., Węsławski, J. M., Dragańska-Deja, K., Wochna, A., Goc, M., and Iliszko, L.: Subglacial discharges create fluctuating foraging hotspots for sea birds in tidewater glacier bays, Scientific Reports, 7, https://doi.org/10.1038/srep43999, 2017.

Vacquié-Garcia, J., Lydersen, C., Ims, R. A., and Kovacs, K. M.: Habitats and movement patterns of white whales Delphinapterus leucas in Svalbard, Norway in a changing climate, Movement Ecology, 6, https://doi.org/10.1186/s40462-018-0139-z, 2018.

Van As, D., Andersen, M. L., Petersen, D., Fettweis, X., Van Angelen, J. H., Lenaerts, J. T. M., Van Den Broeke, M. R., Lea, J. M., Bøggild, C. E., Ahlstrøm, A. P., and Steffen, K.: Increasing meltwater discharge from the Nuuk region of the Greenland ice sheet and implications for mass balance (1960–2012), Journal Of Glaciology, 60, 314–322, https://doi.org/10.3189/2014jog13j065, 2014.

Formatted: English (United Kingdom)

Formatted: English (United Kingdom)

Van Genuchten, C. M., Rosing, M. T., Hopwood, M. J., Liu, T., Krause, J., and Meire, L.: Decoupling of particles and dissolved iron downstream of Greenlandic glacier outflows, Earth And Planetary Science Letters, 576, 117234, https://doi.org/10.1016/j.epsl.2021.117234, 2021.

Van Genuchten, C. M., Hopwood, M. J., Liu, T., Krause, J., Achterberg, E. P., Rosing, M. T., and Meire, L.: Solid-phase Mn speciation in suspended particles along meltwater-influenced fjords of West Greenland, Geochimica Et Cosmochimica Acta, 326, 180–198, https://doi.org/10.1016/j.gca.2022.04.003, 2022.

Van Heukelem, L. and Thomas, C. S.: Computer-assisted high-performance liquid chromatography method development with applications to the isolation and analysis of phytoplankton pigments, Journal Of Chromatography A, 910, 31–49, https://doi.org/10.1016/s0378-4347(00)00603-4, 2001.

Wang, Y., Gélinas, Y., De Vernal, A., Mucci, A. O., Allan, E., Seidenkrantz, M.-S., and Douglas, P. M. J.: High rates of marine organic carbon burial on the southwest Greenland margin induced by Neoglacial advances, Communications Earth & Environment, 5, https://doi.org/10.1038/s43247-024-01508-2, 2024.

Watts, E. G., Hylén, A., Hall, P. O. J., Eriksson, M., Robertson, E. K., Kenney, W. F., and Bianchi, T. S.: Burial of Organic Carbon in Swedish Fjord Sediments: Highlighting the Importance of Sediment Accumulation Rate in Relation to Fjord Redox Conditions, Journal Of Geophysical Research Biogeosciences, 129, https://doi.org/10.1029/2023jg007978, 2024.

Wehrmann, L. M., Formolo, M. J., Owens, J. D., Raiswell, R., Ferdelman, T. G., Riedinger, N., and Lyons, T. W.: Iron and manganese speciation and cycling in glacially influenced high-latitude fjord sediments (West Spitsbergen, Svalbard): Evidence for a benthic recycling-transport mechanism, Geochimica Et Cosmochimica Acta, 141, 628–655, https://doi.org/10.1016/j.gca.2014.06.007, 2014.

Winkelmann, D. and Knies, J.: Recent distribution and accumulation of organic carbon on the continental margin west off Spitsbergen, Geochemistry Geophysics Geosystems, 6, https://doi.org/10.1029/2005gc000916, 2005.

Włodarska-Kowalczuk, M., Mazurkiewicz, M., Górska, B., Michel, L. N., Jankowska, E., and Zaborska, A.: Organic Carbon Origin, Benthic Faunal Consumption, and Burial in Sediments of Northern Atlantic and Arctic Fjords (60–81°N), Journal Of Geophysical Research Biogeosciences, 124, 3737–3751, https://doi.org/10.1029/2019jg005140, 2019.

Wright, S. W., and Jeffrey, S. W.: High-resolution HPLC system for chlorophylls and carotenoids of marine phytoplankton, in: Phytoplankton pigments in oceanography: Guidelines to modern methods, edited by: Jeffrey, S. W., Mantoura, R. F. C., and Wright, S. W., Monographs on Oceanographic Methodology, 10, UNESCO Publishing, Paris, pp. 327–341, ISBN 92-3-103275-5, 1997.

Zaborska, A., Włodarska-Kowalczuk, M., Legeżyńska, J., Jankowska, E., Winogradow, A., and Deja, K.: Sedimentary organic matter sources, benthic consumption and burial in west Spitsbergen fjords – Signs of maturing of Arctic fjordic systems?, Journal Of Marine Systems, 180, 112–123, https://doi.org/10.1016/j.jmarsys.2016.11.005, 2018.